

Chemical Kinetics on Extrasolar Planets

Julianne I. Moses

Space Science Institute, 4750 Walnut Street, Suite 205, Boulder, CO, 80301, USA

Chemical kinetics plays an important role in controlling the atmospheric composition of all planetary atmospheres, including those of extrasolar planets. For the hottest exoplanets, the composition can closely follow thermochemical-equilibrium predictions, at least in the visible and infrared photosphere at dayside (eclipse) conditions. However, for atmospheric temperatures $\lesssim 2000$ K, and in the uppermost atmosphere at any temperature, chemical kinetics matters. The two key mechanisms by which kinetic processes drive an exoplanet atmosphere out of equilibrium are photochemistry and transport-induced quenching. We review these disequilibrium processes in detail, discuss observational consequences, and examine some of the current evidence for kinetic processes on extrasolar planets.

Key words: extrasolar planets; exoplanets; planetary atmospheres; atmospheric chemistry; photochemistry; chemical kinetics.

1. Introduction

In two short decades, the study of extrasolar planets has evolved from a relatively esoteric, theory-driven, scientific diversion to a full-fledged, observation-driven, vibrant profession [1, 2]. With 859 exoplanets discovered as of January 2013 [3] and thousands more *Kepler* planetary candidates waiting to be confirmed [4, 5], our Sun has lost its status as a unique planetary host. However, each planetary system discovered to date displays its own unique properties, and the sheer diversity of those properties is staggering. Most of the known exoplanets are expected to possess atmospheres of some sort, but those atmospheres will be equally diverse and often have no Solar-System analogs. Can we use basic physical and chemical principles to predict the characteristics and behavior of exoplanet atmospheres? How good are our predictions, and what do we learn from comparisons of observations and theory?

Current observational techniques used to analyze exoplanet atmospheres include direct imaging [6-8] and transit and eclipse measurements [9-12]. Because exoplanets are so much fainter than their host stars, atmospheric characterization by direct imaging is so far only viable for young, bright, hot planets that orbit relatively far from their host stars, and concrete information on atmospheric composition has only recently been reported from this technique [13-21]. Transit and eclipse observations, where light from the system is observed to dim as the planet passes in front of and behind the host star as seen from the observer, have been more fruitful in determining atmospheric composition, but observational biases still limit the types of planets that can be studied in this manner. Transits have a higher probability of being observed for planets orbiting very close to their host stars, and the signal is stronger for larger planets. Therefore, close-in giant planets — the so-called “hot Jupiters” and “hot Neptunes” — currently

dominate exoplanet atmospheric observations, and our review of exoplanet chemistry will focus on such planets. Transit and eclipse observations have enabled the first-ever detections of neutral and ionized atoms like Na, H, O, C⁺, Si⁺⁺, Mg⁺, and K [9,22-26] and molecules like H₂O, CH₄, CO₂, and CO [27-36] in exoplanet atmospheres.

The first-order properties of exoplanet atmospheres can be predicted theoretically based on the planet's mass, internal heat flux (and/or age), assumed bulk elemental composition, and incident stellar flux [37]. Given these basic parameters, models of thermochemical equilibrium, cloud condensation, and radiative and convective energy transport can be used to predict the composition and thermal structure within the planet's atmosphere, as well as with the observable spectral behavior [38-46]. Chemical equilibrium is a convenient starting point for these types of calculations, as the abundances of individual species can be calculated in a straightforward manner for any given temperature, pressure, and elemental composition through minimization of the Gibbs free energy of the system [39, 42]. The actual pathways (e.g., chemical reactions) required to achieve that equilibrium do not matter, nor does the history of the system, greatly simplifying the calculations. At high temperatures, such as within the deep atmospheres of hot Jupiters, chemical reactions can overcome energy barriers to proceed equally well in both the forward and reverse direction, and the chemical equilibrium assumption is justified. However, for cooler regions of the atmosphere or when incident ultraviolet photons or high-energy ionizing/dissociating particles are present, chemical equilibrium becomes more difficult to achieve, and chemical kinetics or other disequilibrium mechanisms can control the composition.

The two main kinetics-related disequilibrium processes expected to modify abundances within exoplanet atmospheres are *photochemistry* and *transport-induced quenching*. Photochemistry refers to the chemical kinetics that results from the absorption of short-wavelength stellar photons or high-energy corpuscular radiation like cosmic rays. Transport-induced quenching refers to the mechanism by which the atmospheric composition is driven away from chemical equilibrium as a result of the dominance of transport processes like convection or large-scale "eddy" diffusion (e.g., from gravity-wave breaking or wave-driven circulation) over chemical reactions [47-49]. While often considered second-order effects, both of these disequilibrium processes can significantly alter the composition and hence the radiative properties, thermal structure, and even dynamics of the atmosphere, making them important processes to consider in theoretical models. As an example, the photolysis of methane on Jupiter and the other giant planets within our own Solar System leads to the generation of complex hydrocarbons, introducing numerous trace photochemical products to the Jovian stratosphere [e.g., 50]. Some of these products, like C₂H₂ and C₂H₆, become key infrared coolants [51], while some of the more refractory products can condense in the stratosphere to form hazes that absorb sunlight and provide localized heating [52]. The photochemical products strongly influence the spectral behavior, radiative energy transport, and thermal profile, which feed back to affect the stratospheric circulation [e.g., 53]. Due to the intense ultraviolet flux incident onto the atmospheres of close-in transiting exoplanets, photochemistry is expected to play a significant role on hot Jupiters [54-66], although the observable consequences may be restricted to high altitudes in some cases, particularly for the hotter atmospheres. Transport-induced quenching can potentially affect the composition throughout the visible and infrared photosphere of exoplanets [42,62-63,66-72], thereby affecting the thermal structure and spectral behavior.

We review current knowledge of these two disequilibrium processes and discuss how atmospheric properties like the thermal structure, bulk elemental abundance, and transport properties can affect the predicted composition. We also briefly discuss the observational evidence for disequilibrium compositions.

2. Transport-induced quenching

Transport-induced quenching within giant-planet atmospheres was first described by Prinn and Barshay [47] to explain the observed ~ 1 part per billion (ppb) abundance of CO in Jupiter’s upper troposphere, despite the negligible amount expected at local temperature-pressure conditions from chemical-equilibrium arguments. As a parcel of gas is transported through the atmosphere, the mole fraction of a constituent can become “quenched” when transport time scales drop below the chemical kinetics time scales required to maintain that constituent in equilibrium with other species. The mole fraction of that species then remains fixed at that quenched abundance. Quenching typically occurs when the temperature of the system drops low enough that reactions no longer occur equally well in both the forward and reverse directions; however, pressure changes can also play a role. The best-studied quenching process is that of CO-CH₄ interconversion due to vertical mixing because of the importance of that process for Solar-System giant planets [47,73-77], brown dwarfs [70-71,78-84], and extrasolar giant planets [17,60,62-63,67,69,85-86]. In fact, CO-CH₄ quenching has particularly important observational consequences for hot Jupiters and brown dwarfs because their atmospheric temperature profiles often cross the boundary between regions in which CH₄ or CO are the dominant carbon constituents, with transport-induced quenching then leading to CO and/or CH₄ mole fractions that are orders of magnitude different from chemical-equilibrium predictions. The resulting spectral implications can be major (see above references). Although time-constant arguments have historically been used to predict the quenched abundances of CO and CH₄, Bézard et al. [76], Moses et al. [62], and Visscher and Moses [71] discuss some of the pitfalls of such techniques that can arise if the underlying assumptions are not sound. Many investigators instead now solve the full continuity equations for a large number of species to track transport-induced quenching [61-63,65-66,71-72,77] a technique that has the added benefit of more accurately predicting the profiles of other potentially spectrally active species (e.g., CO₂, C₂H₂, HCN) once some critical “parent” molecules are quenched.

However, these more sophisticated models are also only as good as their inputs and assumptions, and although the kinetics of the C-H-O system has been well studied due to combustion-chemistry and terrestrial atmospheric-chemistry applications [87-89], the exact mechanism involved with CH₄-CO quenching in reducing environments is not strictly established. As originally hypothesized [47], individual reactions that convert oxidized carbon (e.g., CO, CO₂, HCO, H₂CO, CH₂OH, CH₃O, CH₃OH) to reduced carbon (e.g., CH₄, CH₃, C₂H₂, C₂H₄, C₂H₆) and *vice versa* are of critical importance to the problem, as reactions within the oxidized or reduced families tend to be faster. The reaction $\text{H}_2 + \text{H}_2\text{CO} \rightleftharpoons \text{OH} + \text{CH}_3$ was originally proposed as the rate-limiting step for CO-CH₄ conversion [47, 49, 75], but this reaction is likely too slow under typical brown-dwarf or giant-planet conditions to be a key player in the dominant interconversion mechanism [62,71,74,76-77,80]. Yung et al. [74] suggest that the reaction $\text{H} + \text{H}_2\text{CO} + \text{M} \rightarrow \text{CH}_3\text{O} + \text{M}$ is the rate-limiting step as a potential bottleneck to the necessary conversion of the strong CO bond to a weaker single-bonded C-O species. However,

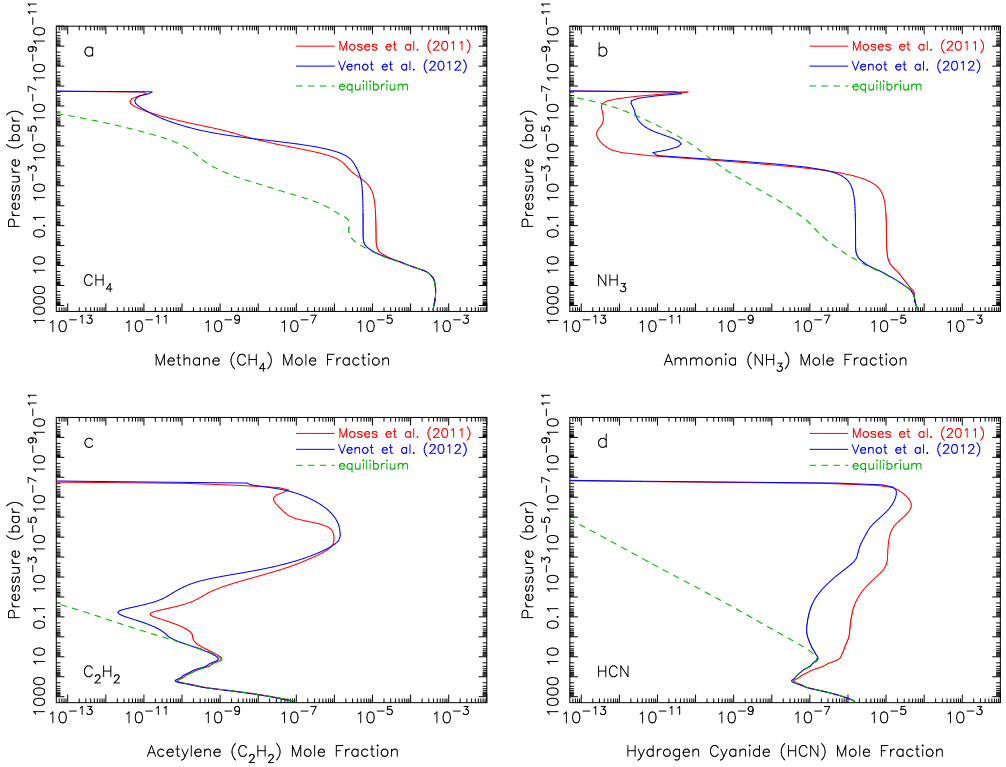


Figure 1. Mole fractions (volume mixing ratios) of (a) CH_4 , (b) NH_3 , (c) C_2H_2 , and (d) HCN from chemical models of HD 189733b, assuming thermochemical equilibrium (green dashed curves), or including photochemical kinetics and transport with the Moses et al. [62] reaction mechanism (red solid curves) or with the Venot et al. [66] reaction mechanism (blue solid curves). The dayside thermal structure and nominal eddy diffusion coefficient profile from [62] were used throughout the modeling [see also 66,90]. Note that the kinetics models begin to diverge from the equilibrium profiles at different depths due to differences in the adopted reaction mechanism. The resulting “quenched” abundances therefore differ between models, despite the same assumptions concerning atmospheric transport. See Venot et al. [66] for similar figures. Online version is in color.

more recent studies point to alternative reactions being the rate-limiting steps; the most thorough and updated discussions of the problem are presented in [62, 71].

Figure 1 demonstrates that the quenched abundances of species like CH_4 and NH_3 are very sensitive to the individual reactions and rate coefficients in the adopted reaction mechanism for these kinetics-transport models. Moreover, once molecules like CH_4 and NH_3 quench, the abundances of other species such as C_2H_2 and HCN can be affected, and the profiles of minor species can become complicated. Because the full reaction mechanisms for the Moses et al. [62] and Venot et al. [66] studies are published online, intercomparisons between these models is relatively straightforward; therefore, we focus our discussion on these two models and apply the mechanisms to the dayside atmosphere of HD 189733b. Venot et al. [66] do not provide a detailed discussion of their dominant $\text{CH}_4 \rightarrow \text{CO}$ quench mechanism, but it is clear that interconversion between these two species is more efficient in their model than in Moses et al. [62], as the CH_4 mole

fraction in the Venot et al. model continues to follow the equilibrium predictions to higher altitudes (lower pressures/temperatures) than in [62]. The resulting quenched CH_4 abundance is therefore lower in the Venot et al. [66] model than in the Moses et al. [62] model.

A detailed examination of the two mechanisms reveals that the main difference with respect to the CH_4 quench behavior derives from the adopted rate coefficients for the reaction $\text{H} + \text{CH}_3\text{OH} \rightarrow \text{CH}_3 + \text{H}_2\text{O}$. The Venot et al. mechanism originates from combustion-chemistry studies that use the Hidaka et al. [91] rate-coefficient estimate for this reaction; some previous giant-planet quenching studies also initially adopted this rate coefficient [77]. However, as is discussed by Visscher et al. [77] and Moses et al. [62], the $\text{H} + \text{CH}_3\text{OH} \rightarrow \text{CH}_3 + \text{H}_2\text{O}$ reaction likely proceeds with a very large energy barrier and is therefore much slower than was estimated by [91]. When a more realistic rate coefficient for this reaction, as calculated from *ab initio* transition-state theory [62], is incorporated into the Venot et al. mechanism, the resulting quenched CH_4 mole fraction is more in line with that of Moses et al. [62], with remaining differences being largely due to the adoption of a larger rate coefficient for $\text{H}_2\text{O} + {}^1\text{CH}_2 \rightarrow \text{CH}_3\text{OH}$ in the Venot et al. model (which was again seems to be based on an estimate [e.g., 91]) than in the Moses et al. model (where the rate-coefficient calculations of [93] have been adopted).

Although we think that CH_4 -CO quenching is unlikely to proceed exactly as is described by the Venot et al. mechanism, due to some problems with individual rate coefficients discussed above, it is possible that other reactions and/or rate coefficients not considered by either [62] or [66] (or any other investigations) could be dominating on hot Jupiters. As an example, Hidaka et al. [91] favored a fast rate for $\text{H} + \text{CH}_3\text{OH} \rightarrow \text{CH}_3 + \text{H}_2\text{O}$ precisely because they were looking for an effective way to reproduce the observed yield of CH_4 in their methanol decomposition experiments. If that reaction is not responsible, as we indeed suggest it is not, then other reactions must be taking up the slack, and it remains to be demonstrated whether any of the updated reaction rate coefficients in the Moses et al. [62], Venot et al. [66] mechanisms, or those of other investigations [59, 61, 65], can reproduce all available experimental data. The quenched abundance of CH_4 should therefore be considered only accurate to within a factor of ~ 2 due to kinetics uncertainties, with other factors such as atmospheric transport properties and thermal structure contributing additional uncertainty. It is obvious from Fig. 1, however, that CO- CH_4 quenching matters on HD 189733b and likely other close-in hot Jupiters, with potential observable consequences, just as on brown dwarfs and directly-imaged extrasolar giant planets [13,17,70,79,81]. The colder the exoplanet atmosphere, the deeper the quench point, and the larger the quenched CH_4 mole fraction that could be present in the visible-infrared photosphere [62].

Similarly, interconversion between the main nitrogen species N_2 and NH_3 can be kinetically inhibited in planetary and brown-dwarf atmospheres [49,94-97], leading to quenching of both species. The N_2 - NH_3 quench point likely occurs deeper in the atmosphere than the CO- CH_4 quench point, but the kinetics of nitrogen species under high-temperature, high-pressure, reducing conditions is even more uncertain than that of carbon and oxygen. The key to the kinetics of interconversion of N_2 and NH_3 is likely the reduction of the strongly triple-bonded N_2 into progressively weaker N-N bonded N_2H_x species, followed by thermal decomposition or disproportionation reactions converting the N_2H_x molecule into two NH_x species. Initial suggestions for the rate-limiting steps in the process [75,94-95], such as $\text{N}_2 + \text{H}_2 \rightleftharpoons 2\text{NH}$ have given

way to other suggestions because the above reaction will likely be too slow to play any significant role in the $\text{N}_2\text{-NH}_3$ conversion [97]. Alternative suggestions for the rate-limiting step in NH_3 quenching include (a) $\text{N}_2\text{H}_3 + \text{M} \rightleftharpoons \text{H} + \text{N}_2\text{H}_2 + \text{M}$ [97], where M is any additional atmospheric species in this three-body reaction, (b) $2\text{NH}_2 \rightleftharpoons \text{N}_2\text{H}_2 + \text{H}_2$ [61], and (c) $\text{NH} + \text{NH}_2 \rightleftharpoons \text{N}_2\text{H}_2 + \text{H}$ [62]. These are all viable possibilities, and published rate coefficients for these reactions or their reverses are available from theoretical calculations [98-101] or experiments [102], but large uncertainties and discrepancies for these and other potentially important reaction rate coefficients exist in the literature. The predicted quenched abundance of NH_3 on HD 189733b differs by about an order of magnitude when using the Venot et al. [66] versus the Moses et al. [62] reaction mechanism (see Fig. 1 and [66]), and Venot et al. [66] have tested several other combustion-based reaction mechanisms, all which predict different quenched NH_3 abundances on HD 189733b. These differences emphasize the kinetic uncertainties that currently plague quench predictions for nitrogen species.

Kinetic interconversion between N_2 and NH_3 is clearly much more effective in models that use the Venot et al. [66] mechanism as opposed to the Moses et al. [62] mechanism. Ammonia diverges from the equilibrium profile much deeper with the Moses et al. [62] mechanism, and although the NH_3 does not truly quench until higher altitudes due to transport time scales being only slightly smaller than the kinetic conversion time scales in the nearly isothermal region between a few bars and ~ 0.1 kbar in the HD 189733b model [62], the resulting quenched NH_3 abundance is significantly greater in the Moses et al. [62] model than the Venot et al. [66] model. The main differences appear to be related to reactions of NH_2 with NH_2 and/or NH_3 . Venot et al. [66] have adopted very large rate coefficients for some reactions that convert NH_2 to N_2H_x species based on the work of Konnov and De Ruyck [103, 104]. For example, the Venot et al. rate coefficient for $\text{NH}_2 + \text{NH}_3 \rightarrow \text{N}_2\text{H}_3 + \text{H}_2$ (based on [103]) is more than three orders of magnitude larger at 1600 K than the expression used in Moses et al. [62] (based on [105]), and this reaction plays a major role in the efficient interconversion of $\text{NH}_3 \rightleftharpoons \text{N}_2$ in the Venot et al. [66] mechanism. However, the rate-coefficient expression advocated by Konnov & De Ruyck [103] is simply an *ad hoc* eight-fold reduction of a previous estimate [106], which Konnov & De Ruyck altered to keep that reaction from having any adverse effects on their experimental simulations [103]. As such, the Konnov & De Ruyck expression is more of an upper limit than a true recommendation. In fact, the $\text{NH}_2 + \text{NH}_3 \rightarrow \text{N}_2\text{H}_3 + \text{H}_2$ reaction likely has a significantly higher barrier than the Konnov & De Ruyck expression indicates, and the reaction is not expected to be important under conditions relevant to hydrazine combustion or ammonia pyrolysis [105]. It is also unlikely to be important for $\text{NH}_3\text{-N}_2$ quenching in giant-planet atmospheres if the rate coefficient has an energy barrier similar to that suggested by Dean et al. [105] (see also [62]); however, further rate-coefficient information on this reaction is needed before it can truly be ruled out as a participant in the $\text{NH}_3 \rightleftharpoons \text{N}_2$ interconversion process. The adoption of a fast rate coefficient for this reaction strongly influences the low derived NH_3 abundance in the Venot et al. model.

The $\text{NH}_2 + \text{NH}_2 \rightarrow \text{N}_2\text{H}_2 + \text{H}_2$ reaction represents a more interesting case, as the product pathways and rate coefficients are not well known for the $\text{NH}_2 + \text{NH}_2$ reaction. Venot et al. [66] adopt a relatively large rate coefficient for this reaction based on Konnov & De Ruyck [104], which in turn was influenced by the experimental study of Stothard et al. [102] that indicates that N_2H_2 (as an unidentified isomer) is an important product in the $\text{NH}_2 + \text{NH}_2$ reaction at room temperature. Theoretical

models [98-99,101] in contrast, suggest that the standard pathways producing $\text{H}_2 + \text{N}_2\text{H}_2$ (various isomers) are relatively unimportant at room temperature. In the Klippenstein et al. [98] calculations, for instance, two NH_2 radicals interact on a singlet potential energy surface via barrierless addition (i.e., to form N_2H_4), with the stabilization of the adduct dominating especially at low temperatures and high pressures, or potential elimination of H and H_2 occurring at higher temperatures (e.g., to form $\text{H} + \text{N}_2\text{H}_3$ or $\text{H}_2 +$ various isomers of N_2H_2). On the triplet surface, the $\text{NH}_2 + \text{NH}_2$ reaction can occur via hydrogen abstraction to form $\text{NH} + \text{NH}_3$ [98], which is especially important at high temperatures. The barriers leading to $\text{H}_2 + \text{N}_2\text{H}_2$ are sufficiently high on the singlet surface in the Klippenstein et al. [98] models that the product channels forming various isomers of N_2H_2 are unimportant even at the moderately high temperatures relevant to NH_3 quenching on the giant planets (1500-2100 K). Moses et al. [62] have adopted the rate-coefficient recommendations of Dean & Bozzelli [99] for the H_2 elimination pathways, which are more in line with the Klippenstein et al. [98] recommendations than the Konnov & De Ruyck [104] recommendations, and the resulting $\text{NH}_2 + \text{NH}_2 \rightarrow \text{N}_2\text{H}_2 + \text{H}_2$ or $\rightarrow \text{H}_2\text{NN} + \text{H}_2$ pathways are not very important in $\text{NH}_3 \rightarrow \text{N}_2$ conversion in their HD 189733b and HD 209458b models. On the other hand, Asatryan et al. [101] suggest that there could be a potential low-energy pathway to $\text{NH}_2 + \text{NH}_2 \rightarrow \text{cis-N}_2\text{H}_2 + \text{H}_2$ that could occur through an “activated” N_2H_4 intermediate even at moderately low temperatures. Stereoselective attack of *cis*- N_2H_2 by H_2 then leads to $\text{N}_2 + 2\text{H}_2$ with a comparatively low barrier. As mentioned by Altinay & Macdonald [107], this suggested pathway needs further theoretical verification, but if plausible, it might lead to a more efficient means to $\text{NH}_3 \rightarrow \text{N}_2$ conversion in exoplanet atmospheres than has been implemented in the Moses et al. model.

In all, the Moses et al. [62] and Venot et al. [66] mechanisms can be considered to bracket the low and high ends of possible $\text{NH}_3 \rightleftharpoons \text{N}_2$ conversion efficiencies, and the expected quenched NH_3 abundance on transiting exoplanets is uncertain by about an order of magnitude (see also Venot et al. [66]). To improve that situation, we need reliable rate coefficients for several reactions involving NH_x and N_2H_x species at temperatures of ~ 1500 -2200 K and pressures of ~ 1 -1000 bar. Of particular interest are rate coefficients for the various possible pathways involved with the reactions of $\text{NH}_2 + \text{NH}_2$, $\text{NH}_2 + \text{NH}_3$, $\text{NH} + \text{NH}_2$, $\text{NH} + \text{NH}_3$, $\text{H}_2 + \text{N}_2\text{H}_2$ (various isomers), $\text{H}_2 + \text{N}_2\text{H}_3$, $\text{H} + \text{N}_2\text{H}_x$, and thermal decomposition of N_2H_4 , N_2H_3 , and various N_2H_2 isomers. Since the chemistry of ammonia and hydrazine is also important on Jupiter and Saturn, extension to ~ 100 K temperatures would also be valuable for investigation of tropospheric photochemistry on those planets.

Carbon monoxide and molecular nitrogen also technically quench when CO-CH_4 and $\text{N}_2\text{-NH}_3$ interconversion reactions cease to be able to compete with vertical transport processes. However, because these molecules are the dominant carbon and nitrogen constituents at the quench points in the HD 189733b and HD 209458b models [62, 66], the quenching behavior for these species is less obvious since their equilibrium mole fractions are expected to remain constant to higher altitudes anyway. If the quench points on exoplanets were to occur in a region where both the CH_4 and CO (or N_2 and NH_3) have similar abundances, then the quenching of both species would be more obvious.

Once major molecules like NH_3 and CH_4 are quenched, the abundance of other species can be strongly affected. For example, Fig. 1 illustrates that the HCN and C_2H_2 abundances depart from equilibrium when NH_3 and CH_4 quench on HD 189733b, and these molecules continue to react with the quenched “parent” molecules up to higher

altitudes, causing their column abundances to greatly exceed equilibrium predictions. Acetylene maintains a pseudo-equilibrium with H_2 and quenched CH_4 up ~ 0.1 bar in this model (see [62] for more information about the important reaction schemes). The large bulge in the C_2H_2 abundance at higher altitudes is due to photochemical and disequilibrium thermochemical kinetics processes. Similarly, HCN maintains a pseudo-equilibrium with quenched NH_3 and CH_4 (with a net reaction $\text{NH}_3 + \text{CH}_4 \rightleftharpoons \text{HCN} + 3\text{H}_2$, see Moses et al. [62] for detailed reaction schemes) to ~ 0.1 mbar, above which the downward transport of photochemically produced HCN dominates the profile. Transport-induced quenching can therefore affect species abundances even before their own quench points are reached, and full kinetics models are needed to describe this behavior.

Quenching does not occur solely in the vertical direction. Possible horizontal quenching was first discussed by Cooper & Showman [67]. Time-constant arguments [67, 62] indicate that horizontal winds have the potential to transport gas species to cooler atmospheric regions before the species have time to equilibrate, which could particularly affect transit observations of the cooler terminator regions. Similarly, quenching (vertical or horizontal) can affect the atmospheric composition of close-in eccentric exoplanets [108] such that the large swings in temperature over the orbit may not necessarily be accompanied by large changes in atmospheric composition if orbital time scales are shorter than chemical reaction time scales. Agúndez et al. [72] have followed up these ideas with a more sophisticated kinetics model to investigate horizontal quenching on HD 209458b under the simplifying assumptions of constant zonal winds as a function of altitude, latitude, and longitude, with no photochemistry or vertical transport included; they find that horizontal quenching is indeed very important, especially at pressures less than ~ 0.1 bar (depending on the species). The horizontal quenching suppresses longitudinal abundance gradients, greatly reducing dayside vs. terminator abundance differences, with resulting major observational consequences. Essentially, Agúndez et al. [72] find that abundances above the ~ 0.1 bar level are quenched horizontally to dayside equilibrium values, whereas quenching due to vertical mixing controls the abundances at deeper levels down to the quench point. The resulting terminator and nightside abundance profiles differ from models based on either thermochemical equilibrium or kinetics considering vertical transport only, and the main prediction is a reduction in the mid-to-high altitude abundance of species like CH_4 and NH_3 that are relatively unstable at the high dayside temperatures of HD 209458b but that would nominally be stable at cooler terminator and nightside temperatures.

Clearly, the chemical profiles in the 3D situation will be complicated, and kinetics and transport-induced quenching in both the vertical and horizontal direction must be considered to accurately reflect the situation in the real atmosphere. The inclusion of vertical mixing in such longitudinally variable models is an important next step, as it would more realistically capture the dayside abundances of vertically quenched species like NH_3 and CH_4 , and thus more accurately predict the horizontally quenched terminator and nightside abundances. The addition of photochemistry to the problem will complicate things further, as photochemical time constants tend to be very short in the upper atmospheres of these planets. Ultimately, it will be valuable to move toward the inclusion of more sophisticated kinetics directly within the 3D general circulation models, as the disequilibrium constituents can affect the radiative properties of the atmosphere, and the resulting feedback on the temperatures and even dynamics could be important.

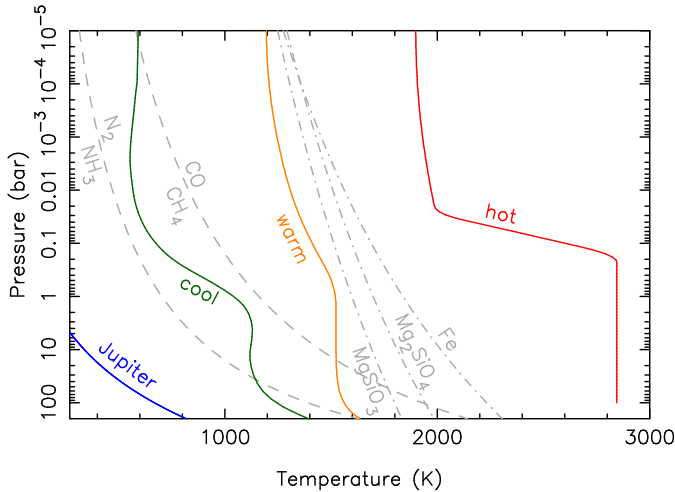


Figure 2. Thermal profiles for the hypothetical “hot”, “warm”, and “cool” exoplanets (as labeled) used in the chemical models shown in Fig. 3. The gray dashed lines represent the equal-abundance curves for CH_4 - CO and NH_3 - N_2 . Profiles to the right of these curves are within the N_2 and/or CO stability fields. The dot-dashed lines show the condensation curves for MgSiO_3 , Mg_2SiO_4 , and Fe (solid, liquid) [112]. Online version is in color.

3. Photochemistry

The consequences of photochemistry on the atmospheric composition of exoplanets have been explored by numerous groups [54-66,109]. We briefly review how photochemistry affects the carbon, nitrogen, and oxygen species in the 0.1-1000 mbar region of hot Jupiters and hot Neptunes, i.e., the pressure region at which the infrared transit and eclipse observations have their highest sensitivity. Higher-altitude thermospheric photochemistry is discussed by [56-58], and sulfur photochemistry is discussed by [59]. Little work has yet been done on the photochemistry of other elements like phosphorus, alkalis, or metals due to a lack of relevant kinetic information.

Although stellar UV photons are the ultimate instigators of photochemistry, the resulting abundances of the observable photochemical products on hot Jupiters depend less on the magnitude of the incident UV flux than on the overall atmospheric thermal structure (and hence the stellar flux in the visible and near-IR) because of the high sensitivity of the “parent” molecule abundances to temperature. Near-solar composition atmospheres that are hotter than ~ 1600 K in the 0.1-1000 mbar region will contain CO , H_2O , and N_2 as their dominant heavy molecular constituents. These molecules are relatively stable against photochemical destruction and/or tend to recycle efficiently (e.g., [62]) so that photochemistry does not remove them from the 0.1-1000 mbar region (unless temperatures are so high that these molecules, too, become unstable). Cooler atmospheres will contain more CH_4 and NH_3 , which are more interesting from a photochemical standpoint.

Examples of the influence of atmospheric temperatures on the photochemical composition are shown in Figs. 2 & 3. First, we present the thermal profiles of three hypothetical “hot,” “warm,” and “cool” exoplanets in Fig. 2, along with some important chemical-equilibrium boundaries. Although these temperatures are based on published

profiles for specific exoplanets [63,110-111], we use them generically here for the photochemical models shown in Fig. 3, which all assume a solar composition of elements and an arbitrary constant-with-altitude eddy diffusion coefficient of $10^9 \text{ cm}^2 \text{ s}^{-1}$. The assumed incident stellar flux in the models, however, remains consistent with the adopted thermal structure, so that the hot planet is receiving a larger overall incident flux. Note from Fig. 2 that the thermal profile of “cool” exoplanet lies in a regime in which CH_4 is the dominant carbon species throughout much of the atmosphere except at very low pressures, whereas the profile transitions from the NH_3 regime to the N_2 regime deeper in the atmosphere; the thermal profile of the “warm” exoplanet lies in the N_2 -dominated regime, but crosses the equal-abundance boundary between CO and CH_4 near 10 bar; and the thermal profile for the “hot” planet lies solidly within the N_2 and CO stability regimes. The location of the thermal profile within these chemical stability boundaries controls what “parent” molecules are available to initiate photochemistry. Figure 3 then shows the expected composition from the consideration of either thermochemical equilibrium (left side of plot) or disequilibrium chemistry due to thermochemical and photochemical kinetics and vertical transport (right side of plot), using the models described in Moses et al. [62, 63].

One obvious consequence of photochemistry on all of these close-in exoplanets, regardless of the thermal structure, is the huge production rate of H at high altitudes (due to H_2 photolysis, H_2 thermal decomposition in the planet’s expected hot thermosphere, and H_2O photolysis and subsequent catalytic destruction of H_2). The atomic H then diffuses downward to affect the chemistry of other molecules. The catalytic H_2O photolysis source of H was first described by [54]. Similar catalytic destruction mechanisms involving CH_4 and NH_3 [62] operate in the cool and warm exoplanet atmospheres where these molecules are more abundant. Atomic H is expected to become the dominant atmospheric constituent at relatively high (\sim microbar) pressures, with the exact transition from H_2 to H depending on the soft x-ray and EUV flux from the host star, thermospheric temperatures, and hydrodynamic winds [57]. Hydrodynamic descriptions and ion chemistry are needed to accurately model the chemical behavior at altitudes above $\sim 1 \mu\text{bar}$ on highly irradiated planets [56, 57], so the high-altitude results presented here are phenomenological only. Neutral O, C, and N from the photodestruction of CO, N_2 , and H_2O are undoubtedly going to be important at high altitudes on highly irradiated planets, but hydrodynamic winds likely drag these atomic constituents to higher altitudes than are shown in this hydrostatic model.

On very hot exoplanets, like our “hot” generic giant planet shown in Fig. 3, photochemistry is relatively unimportant [see also 62-63,65]. Photolysis of CO and N_2 leads to the high-altitude production of atomic species like C and N that are not predicted to be important under equilibrium conditions. Such atomic species (as well as O) and their ions could be observable in UV transit observations (e.g., [23]). At high altitudes, hydroxyl radicals (OH) are also produced from H_2O photolysis or reaction with atomic H, and HCN is produced from CO and N_2 photolysis through schemes such as are described at the beginning of Section 3.5 of Moses et al. [62], but neither of these species remain stable in regions where atomic H dominates. Some production of NO (peaking at ppm abundances) and even O_2 (peaking at 10 ppb abundances) occurs, but these species are confined to a narrow altitude region where CO and N_2 photolysis is effective (i.e., before CO and N_2 self shield) and will not be abundant enough to be observable for solar-composition atmospheres. In fact, virtually all of the interesting photochemistry is confined to this narrow altitude region where the CO and N_2 photolysis rates peak.

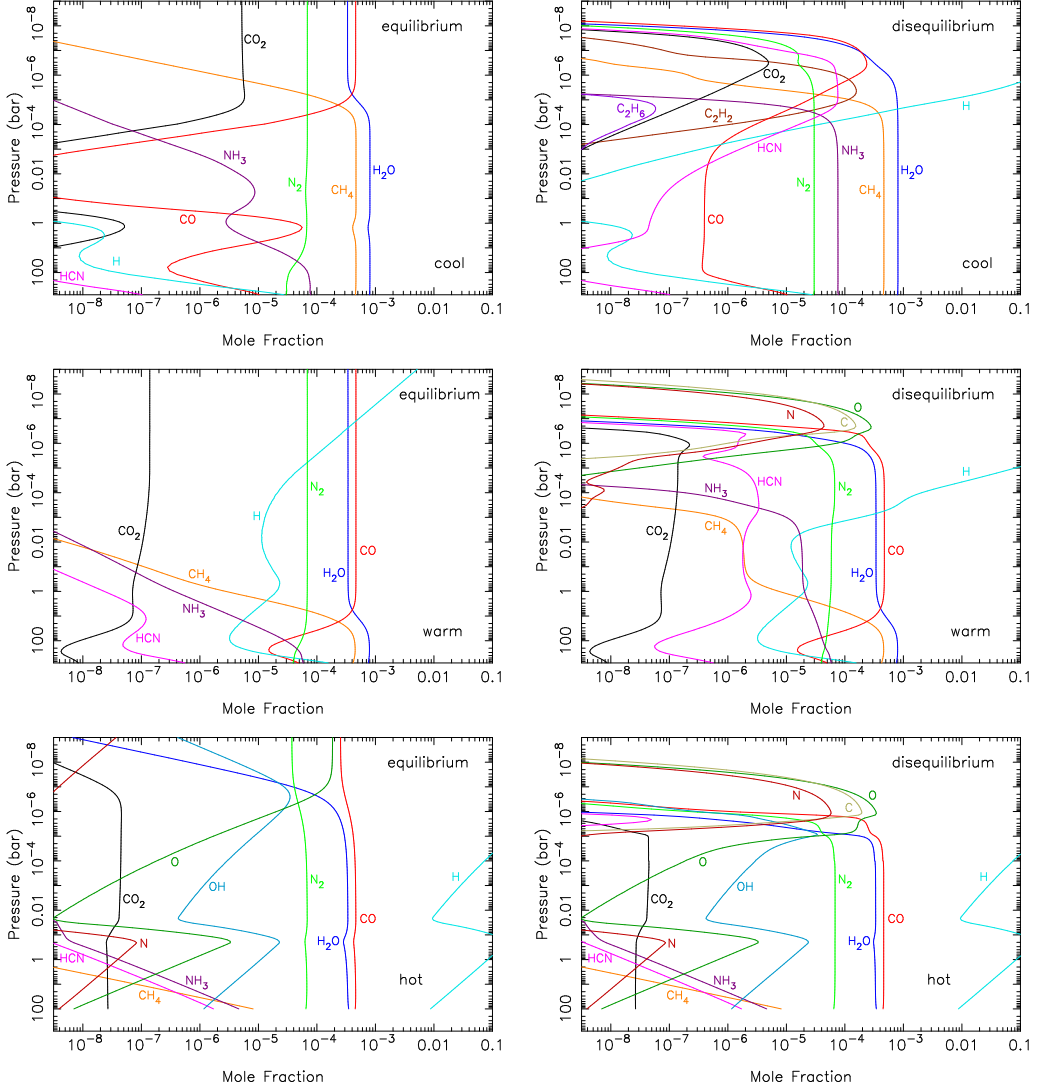
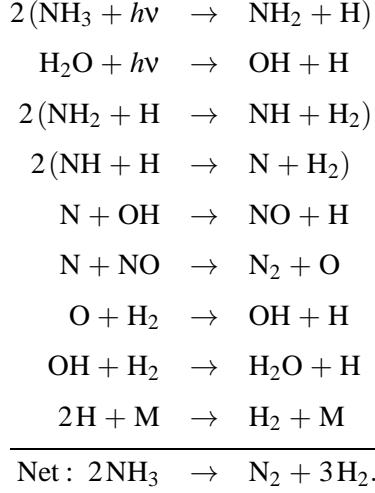


Figure 3. Mole fraction (volume mixing ratio) profiles for our generic cool (top), warm (middle), and hot (bottom) exoplanets, assuming thermochemical equilibrium (left) or thermochemical and photochemical kinetics and transport (right). All models assume a solar elemental composition, and the transport models assume a uniform eddy diffusion coefficient of $10^9 \text{ cm}^2 \text{ s}^{-1}$. Note the decrease in the importance of CH_4 and NH_3 going from the “cool” to the “hot” exoplanet. Online version is in color.

Although H_2O photolysis continues to much deeper levels, the photolysis products tend to recycle rapidly back to H_2O in the H_2 -dominated atmosphere. Temperatures are high enough throughout the bulk of the infrared photosphere at ~ 0.0001 -1 bar such that kinetic reactions can maintain equilibrium, despite the perturbing influence of photolysis of H_2O and other less-abundant species. For the hottest planets, the reaction rates are fast enough that vertical transport-induced quenching is not important either, for reasonable assumptions about vertical eddy diffusion coefficients. If quenching occurs at all, it occurs at high altitudes (low pressures), where the abundance of photochemically active molecules like NH_3 and CH_4 have very low equilibrium abundances and so are not major players in the subsequent chemistry. Thermochemical equilibrium is therefore a reasonable assumption for the atmospheric composition of the hottest hot Jupiters, although horizontal quenching may still occur if longitudinal thermal gradients are expected to be large (i.e., the terminator abundances may not necessarily be in equilibrium). There is no specific critical temperature at which disequilibrium processes cease to be important, as the disequilibrium species gradually phase out with increasing temperature, and the results depend on transport processes as well, but both photochemistry and transport-induced quenching become less and less important with increasing effective temperature of the planet and can be safely ignored for photospheric temperatures $\gtrsim 2000$ K.

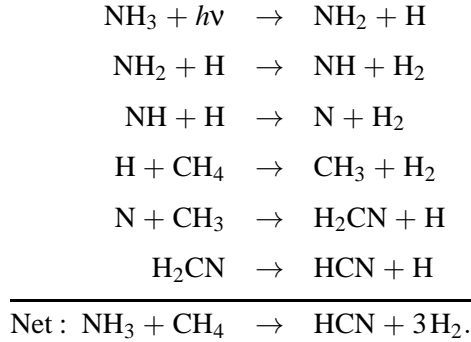
For our “warm” generic exoplanet shown in Fig. 3, both photochemistry and transport-induced quenching are more important than on the hotter exoplanet. Although the relatively stable molecules CO , H_2O , and N_2 remain the dominant carriers of O, C, and N, the quench points for CH_4 - CO and N_2 - NH_3 interconversion are deeper in the atmosphere (assuming “reasonable” transport parameters) where the NH_3 and CH_4 mole fractions are relatively large. Once quenched, these species are mixed upward into regions where they can be photochemically destroyed. Neither NH_3 nor CH_4 is stable in the large background bath of H atoms diffusing down from higher altitudes; moreover, NH_3 is photolyzed at longer wavelengths than the more abundant CO , H_2O , and N_2 such that NH_3 is not shielded against photolysis, and the longer-wavelength UV photons penetrate to deeper atmospheric levels where ammonia photodissociation is important. Ammonia photolysis and subsequent catalytic destruction of H_2 [62] adds an additional source of H atoms down to ~ 10 mbar in the atmosphere of our warm exoplanet, which leads to the photosensitized destruction of CH_4 , and subsequent coupled photochemistry of NH_3 and CH_4 . Some of the nitrogen from the photodestruction of NH_3 ends up in N_2

(with intermediates like N and even NO) through schemes such as



(3.1)

Some of the nitrogen ends up in HCN through schemes such as



(3.2)

In fact, HCN is the ultimate product of the coupled NH_3 - CH_4 photochemistry, and it becomes an important atmospheric constituent in the infrared photosphere of all but the hottest hot Jupiters. As discussed in the previous section, HCN is also an important thermochemical product that can form in “warm” exoplanets from the kinetics of quenched CH_4 and NH_3 [62] via a pseudo-equilibrium that continues between these species despite the cessation of reactions involved with the N_2 - NH_3 and CO - CH_4 quenching.

Hydrogen cyanide is therefore an important disequilibrium product that has been largely ignored to date by exoplanet spectral modelers (with the exception of [62-64,113-114] despite the fact that HCN will be a major constituent whenever atmospheric temperatures are cool enough that CH_4 and NH_3 quench at significant abundances. For atmospheres with near-solar elemental compositions, HCN is likely to be even more abundant than molecules like CO_2 that are typically considered in spectral models (see Fig. 3).

Acetylene (C_2H_2) is another potentially important disequilibrium product on extrasolar giant planets [55,60-66]. It is not formed efficiently in the “warm” exoplanet model presented here, due to the relatively high stratospheric temperatures adopted for this planet, but it can form in abundance on cooler planets through both CO photolysis at high altitudes, and through schemes initiated by the reaction of photochemically produced H with CH_4 [62]. Acetylene tends to be more prevalent at high altitudes on these planets because at higher pressures it is converted efficiently back to methane (and/or to the more hydrogen-saturated ethane on cooler giant planets).

The photochemistry of oxygen compounds on our generic “warm” exoplanet is comparatively less interesting than that of carbon and nitrogen. Photolysis of carbon monoxide occurs only at very high altitudes, and CO with its strong carbon-oxygen bond, is kinetically stable at lower altitudes once the EUV photons responsible for photodissociation have all been absorbed higher up. Water photolysis continues to lower altitudes, but the photolysis products are efficiently converted back to H_2O as long as sufficient H_2 is present. Thus, both CO and H_2O follow their equilibrium profiles throughout the 0.0001-1 bar photospheric region. Carbon monoxide maintains a kinetic equilibrium with CO and H_2O via the reaction $CO_2 + H \rightleftharpoons CO + OH$ throughout most of the photosphere. Some minor excess CO_2 is produced photochemically at high altitudes due to CO and water photolysis, but the large background H abundance allows efficient recycling back to CO. At lower altitudes, CO_2 can be photolyzed by longer-wavelength UV photons to form primarily $CO + O(^1D)$ or $CO + O$, but the $O(^1D)$ and O react with H_2 to form OH, and the OH reacts with the CO to reform the CO_2 , so CO_2 is photochemically stable, again as long as sufficient H_2 is present. Carbon dioxide therefore maintains its equilibrium abundance throughout the 0.0001-1 bar photospheric region in warm giant-planet atmospheres.

Photochemistry within the atmosphere of our “cool” exoplanet shown in Fig. 3 is fundamentally different from that of warmer planets whose photosphere resides within the CO stability field (e.g., [61, 64]). Methane is now the stable parent molecule for the subsequent carbon photochemistry, and the resulting net production rates for complex hydrocarbons are larger than for the hotter planets. As is discussed by Line et al. [61], C_2H_x species become important photolysis products at high altitudes, although they tend to be converted back to methane at lower altitudes. Coupled NH_3 - CH_4 photochemistry as described above and in Moses et al. [62] and Line et al. [61] is effective, and HCN becomes a major photochemical product both locally at various altitudes and from a column-integrated standpoint. Consistent with Line et al. [61], we expect the CH_4 to remain stable throughout the 0.0001-1 bar infrared photosphere on cooler giant planets. Coupled H_2O - CH_4 photochemistry converts the methane to CO at higher altitudes, but these processes are less effective at lower altitudes due to a lack of production of reactive radicals once H_2O (and CH_4) photolysis shuts down due to H_2O self-shielding at $\sim 10^{-4}$ bar and once H has been scavenged back into stable hydrogen-saturated molecules. There are numerous effective pathways for this coupled H_2O - CH_4 photochemistry: (a) atomic O produced from H_2O photolysis can react with CH_3 , C_2H_2 , C_3H_2 , and C_3H_3 to form carbon-oxygen bonded species that eventually form CO, (b) CH can react with water to form H_2CO and ultimately CO, and (c) C reacts with NO produced from coupled N_2 - H_2O photochemistry to form $N + CO$. The carbon-bearing radicals and molecules involved with the above schemes derive ultimately from the reaction of methane with H released from water photolysis. Some CO_2 is produced from this coupled CH_4 - H_2O photochemistry, but CO_2 itself is photolyzed to produce CO, and the reaction $CO +$

$\text{OH} \rightarrow \text{CO}_2 + \text{H}$ cannot recycle the CO_2 fast enough at these temperatures to maintain the $\text{CO-H}_2\text{O-CO}_2$ equilibrium. Carbon dioxide is therefore not a major photochemical product in this cool-exoplanet model.

Transport-induced quenching does enhance the abundance of CO in the IR photosphere of our “cool” exoplanet, and photochemical production of CO occurs at high altitudes, but the column abundance of CO never rivals that of methane in the infrared photosphere. We therefore agree with the conclusions of Line et al. [61] that disequilibrium processes cannot remove methane in favor of CO and/or CO_2 on cooler, solar-composition, giant planets like GJ 436b.

Due to the prevalence of both NH_3 and CH_4 in cooler giant exoplanets, photochemical production of complex hydrocarbons and nitriles is favored in the atmospheres of these cool planets as compared with hotter planets. Benzene (C_6H_6) and cyanoacetylene (HC_3N), for example (not shown in Fig. 3 for reasons of clarity), both achieve peak mole fractions of $\sim 2 \times 10^{-7}$ in our generic cool exoplanet. While these species will not condense at atmospheric conditions relevant to this planet, continued production of refractory species not considered in this model is likely, and the formation of high-altitude photochemical hazes is therefore more probable on these cooler exoplanets [cf. 55,62,115].

4. Sensitivity of disequilibrium chemistry to transport parameters and bulk elemental ratios

We discussed the sensitivity of disequilibrium chemistry and composition on hot Jupiters to atmospheric temperatures in the previous section; the sensitivity to vertical transport parameters like eddy diffusion coefficients (K_{zz}) is discussed in detail in [62,64,115]. The composition is mainly sensitive to the K_{zz} profile through its influence on the quench pressure in transport-induced quenching, and hence through its effect on the abundance of quenched species. If the quenched species are photochemically active at higher altitudes, there can be important consequences with respect to the resulting abundance of photochemical products like HCN, C_2H_x , and complex hydrocarbons and nitriles. The greater the strength of atmospheric mixing at the quench pressures (i.e., the larger the K_{zz} values), the deeper the quench points will be, and the greater the resulting abundance of quenched disequilibrium species like CH_4 and NH_3 on warm Jupiters. That also leads to greater lower-atmospheric abundances of kinetically dependent species like HCN and C_2H_2 . Similarly, on cooler exoplanets where CH_4 is the dominant carbon species, a greater K_{zz} at the CO-CH_4 quench point leads to a greater quenched abundance of CO. Quenching of NH_3 and/or N_2 is also very sensitive to K_{zz} values on cooler exoplanets, where smaller K_{zz} values could push the quench point into the N_2 -dominated regime, allowing N_2 rather than NH_3 to be the dominant nitrogen component in the upper atmosphere, with a corresponding reduction in the column abundances of all disequilibrium nitrogen species.

The strength of vertical mixing in the upper atmosphere also affects the abundance of photochemically produced constituents. The greater the K_{zz} values in the upper atmosphere, the higher the altitude to which the parent molecules can be carried, with a corresponding increase in the column abundance of species that are produced photochemically at high altitudes. The gradient of the K_{zz} profile can affect how rapidly photochemically produced species are transported downward to their thermochemical

destruction regions and thus the overall column abundance below the high-altitude production region [50, 116].

Bulk elemental abundances within the exoplanet atmosphere also affect the predicted equilibrium and disequilibrium compositions. The metallicity of the atmosphere, for example, can strongly influence the expected chemical-equilibrium abundances of heavy molecules [42,60-62,64,115,117,124]. All molecules that contain heavy elements tend to exhibit an increase in abundance when the metallicity is increased. However, the increase in metallicity (all other parameters being equal) leads to a greater increase in CO in comparison to CH₄ and a greater increase in N₂ in comparison with NH₃, and molecules with three or more heavy nuclei, like CO₂, are even more sensitive to metallicity. The above references all emphasize the potential importance of CO₂ as a probe of the atmospheric metallicity on exoplanets, as an increase in metallicity by a factor of x tends to increase the abundance of CO₂ by a factor of x^2 . Photochemical products such as NO, C₂H_x, or HCN that depend on the abundance of the augmented heavy species tend to also become more abundant as the metallicity increases, although the response of disequilibrium species can sometimes be subtler. For example, Moses et al. [62] find that the quenched CH₄ mole fraction in the infrared photosphere of their HD 189733b model actually decreases when the metallicity is increased by a factor of 10 because the CH₄ → CO conversion schemes become more effective when the H₂O and CO abundances increase, such that CH₄ quenches at higher altitudes where the mole fraction is smaller.

The bulk atmospheric elemental ratios can also strongly affect the composition, both from equilibrium- and disequilibrium-chemistry standpoints. The effect of the C/O ratio on the equilibrium composition has been discussed by [63,65,111,114,118-120]; the disequilibrium chemistry consequences have been discussed by [63, 65]. The C/O ratio strongly influences the abundance of spectrally active molecules like CO₂, H₂O, CH₄, HCN, and C₂H₂, particularly on hot Jupiters that are warm enough that CO is expected to be the dominant form of carbon. For C/O ratios < 1 in thermochemical equilibrium at photospheric pressures, methane rapidly decreases in importance with increasing temperature as more and more of the carbon is sequestered in CO, and species like C₂H₂ and HCN are unimportant at all temperatures. At C/O ratios > 1, methane is less temperature sensitive, and species like HCN and C₂H₂ rapidly gain in importance with increasing temperature such that they eventually become the dominant carriers of carbon behind CO. The resulting effects on the atmospheric spectrum can be major [63,111,114,118]. Other elemental ratios like N/O and C/N will have similar interesting effects that have been less well studied.

5. Observational consequences of disequilibrium chemistry

Both transport-induced quenching and photochemistry will affect the spectral properties of exoplanet atmospheres through the influence on the composition. Some of these spectral consequences for extrasolar giant planets have been discussed by [17,62-64,67,69,72,86,113-114,122-124,126]. On the whole, the effects can be minor (see Fig. 4) because the disequilibrium processes tend not to affect the dominant heavy constituents within the 0.0001-1 bar region (e.g., where CO and H₂O dominate on warmer hot Jupiters, and where H₂O and CH₄ dominate on cooler hot Jupiters), and these dominant species — water in particular — control the spectral properties throughout most of the infrared. The disequilibrium effects are then expected to be mostly apparent

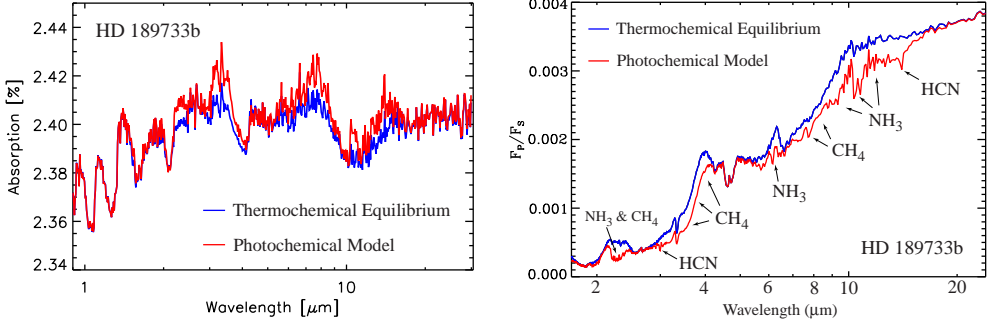


Figure 4. (Left) Synthetic transit spectra for solar-composition HD 189733b models assuming thermochemical equilibrium (blue) or considering thermochemical/photochemical kinetics and transport (red). Absorption depth is plotted as the square of the apparent planet-to-star radius ratio (figure is modified from [62], with spectral calculations from J. J. Fortney). (Right) Synthetic eclipse emission spectra for solar-composition HD 189733b models assuming thermochemical equilibrium (blue) or considering thermochemical/photochemical kinetics and transport (red), plotted in terms of the flux of the planet divided by the flux of the star (figure is modified from [62], with spectral calculations from C. A. Griffith). Disequilibrium molecules responsible for absorption bands in the emission spectrum are labeled specifically. Online version is in color.

within infrared windows where water does not strongly absorb, such as the ~ 1.4 - 1.8 , 2.0 - 2.5 , 3 - 5 , and 8 - 16 μm regions.

One effect that can be less subtle is the consequence of CO - CH_4 quenching on hotter giant planets with strong longitudinal thermal gradients, such that CO is expected to be the dominant thermochemical-equilibrium carbon phase on the dayside, but CH_4 is expected to be the dominant carbon phase at the terminators and/or nightside. As was emphasized by Cooper & Showman [67], CO - CH_4 quenching (both vertical and horizontal) can prevent CH_4 from forming in significant quantities in the cooler regions where equilibrium arguments would expect it to be significant, and the consequences for transit spectra and for predicted spectral variations as a function of orbital phase can be major [67,69,72,124-125]. If CO - CH_4 quenching in high-temperature regions prevents CH_4 from being present in significant quantities in cooler atmospheric regions, the resulting planetary spectrum can exhibit excess opacity in the ~ 2.3 - 2.4 and 4.5 - 4.9 μm wavelength regions, where CO has strong vibrational bands, and reduced opacity in the ~ 2.15 - 2.45 , 3.15 - 3.45 , and 7.2 - 8.2 μm wavelength regions, where CH_4 has strong vibrational bands. Transit and nightside spectra will be particularly sensitive to such CO quenching effects.

On the other hand, vertical quenching of CH_4 can potentially supply methane to both the dayside and terminator photospheres on “warm” Jupiters in excess of what would be expected in equilibrium, particularly if the CO - CH_4 quench point is at or below the base of the “photosphere.” If horizontal thermal gradients still exist at the CO - CH_4 quench point, the final photospheric CH_4 abundance on planets like HD 189733b and HD 209458b will be a complicated function of both vertical and horizontal quenching; however, in essence, vertical quenching will supply methane to the photosphere, and strong horizontal winds and horizontal quenching will help homogenize that methane as a function of longitude. Starting from realistic thermal profiles from general circulation

models [90], Moses et al. [62] find that even in the absence of horizontal quenching, vertical transport-induced quenching supplies a quenched CH_4 mole fraction to the photosphere that only differs by a factor of a few between the terminator and dayside models, compared with the large difference of those disequilibrium predictions in comparison with equilibrium expectations (see Fig. 1). Therefore, transport-induced quenching is expected to provide excess photospheric methane in comparison with equilibrium predictions for both HD 189733b and HD 209458b, with some notable spectral consequences, particularly for the cooler HD 189733b (see [62] and Fig. 4). The main consequence is an increase in absorption at ~ 2.15 - 2.45 , 3 - 4 , and 7 - $9 \mu\text{m}$ from what would be expected based on equilibrium compositions.

Quenching of NH_3 on hot Jupiters over a wide range of temperatures can influence the spectrum by providing additional opacity in the ~ 1.5 , 2.0 , 2.2 - 2.3 , 3.0 , 5.5 - 7.0 , and 8 - $12 \mu\text{m}$ regions, where NH_3 has strong bands. Ammonia and methane quenching provide a thermochemical-kinetics source of HCN, which photochemistry can also enhance in the upper atmosphere. Disequilibrium HCN then provides excess absorption in the ~ 1.53 , 1.85 , 2.8 - 3.1 , 6.5 - 7.5 , and 13 - $16 \mu\text{m}$ wavelength regions, with particularly strong contributions at ~ 3 and $14 \mu\text{m}$. As can be seen from Fig. 4, these disequilibrium nitrogen species can have a notable influence on the exoplanetary spectra within the water-absorption windows, and we encourage the inclusion of HCN and NH_3 in exoplanet spectral models — and encourage the acquisition of high-temperature line parameters for NH_3 and HCN so that spectral modelers can reliably include these species in their calculations.

Acetylene is another photochemical product that can have a potentially important influence on the spectra of cooler planets. Given its predicted abundance on HD 189733b [60, 62, 66], C_2H_2 will not have much of an influence on spectra from that planet (see [62] and Fig. 4), being overshadowed by the more abundant HCN and CH_4 in the ~ 3 and 7 - $8 \mu\text{m}$ regions where C_2H_2 has bands, but acetylene also has several distinct bands in the 1 - $3 \mu\text{m}$ region and the 12.5 - $15 \mu\text{m}$ region (with a strong ν_5 Q branch at $\sim 13.7 \mu\text{m}$) that might provide a unique spectral signature for cooler planets where C_2H_2 is expected to be more abundant. Acetylene will also be a more important constituent for atmospheres with higher C/O ratios [63,65,114], and if there are reasons to expect a high C/O ratio for any given planet [e.g., 63,111,114], both HCN and C_2H_2 should be considered in spectral calculations.

6. Current evidence for disequilibrium chemistry on exoplanets

In the previous section, we discussed some of the expected observational consequences of disequilibrium chemistry on the spectral properties of exoplanets, but it remains to be demonstrated whether actual observations provide any evidence for these effects. Here, we look at some of the existing claims for disequilibrium compositions in the infrared photospheres of extrasolar giant planets and discuss whether photochemistry and transport-induced quenching can account for the observed behavior or whether other processes or atmospheric characteristics must be responsible for that behavior.

Disequilibrium chemistry in the troposphere/stratosphere has been suggested to bring about the following observed hot Jupiter or hot Neptune characteristics:

- *Weak CH_4 absorption on young, directly-imaged giant planets.* Near-infrared spectra and narrow-band photometry suggest that CH_4 -CO quenching occurs

on several of the better-studied directly imaged exoplanets like the those in the HR 8799 system [13-15,17,20-21] and 2M1207b [18]. Quenching of CO at much greater than equilibrium abundances is expected to have important spectral consequences on such planets [127], and indeed is very likely from theoretical grounds, leading to greatly enhanced CO abundances and possible CO/CH₄ ratios greater than unity [17]. Although clouds and potential non-solar metallicities can complicate the interpretation [16, 17, 19, 20], the lack of evidence for strong methane absorption does seem to indicate the occurrence of disequilibrium transport-induced quenching of CO and CH₄ on these planets. This conclusion is further reinforced by recent high-spectral-resolution observations of HR 8799c [21] that show features due to water and CO but not methane.

- *Near-IR detections of CH₄ on HD 189733b and HD 209458b.* Swain et al. [31] report the detection of CH₄ on HD 189733b from transit spectroscopy obtained from the NICMOS instrument on the *Hubble Space Telescope* (HST). The relatively large amount of methane inferred from these observations [31, 34] is in excellent agreement with predictions that include disequilibrium transport-induced quenching of CH₄ [60, 62, 71]. However, the lack of detection of methane (and the corresponding low upper limit) on the dayside of the planet with the same instrument [33] is in conflict with disequilibrium chemistry predictions that include vertical transport [60, 62, 71, 66], making the case for methane via disequilibrium processes inconclusive on HD 189733b. Although photochemical and thermochemical kinetics processes are expected to remove CH₄ from the upper portions of the dayside atmosphere on HD 189733b, the overall column abundance should not be affected much, and transport-induced quenching (both vertical and horizontal) should ensure dayside and terminator methane abundances that differ by only a factor of a few. By the same token, the large dayside abundance of methane inferred from HST/NICMOS eclipse observations of HD 209458b [32] seems too large to be explained by transport-induced quenching [62]; if the spectral signatures are robust, we suggest that alternative (yet to be identified) molecules should be considered as possible candidates for the absorption, or that the atmosphere has a C/O ratio greater than solar. With regard to the latter point, we note that although the *Spitzer* infrared photometric data from eclipse cannot provide meaningful constraints on the CH₄ abundance of HD 209458b [34], the relatively low water abundance inferred from both the HST/NICMOS spectra and *Spitzer* photometric data [32, 34] is also consistent with an inferred high C/O ratio on HD 209458b, but the relatively high derived CO₂ abundance from HST/NICMOS data [32] is not. We conclude that the methane detections on both HD 189733b and HD 209458b do not provide any unambiguous evidence for disequilibrium CH₄ quenching on these planets. Further near-IR observations, especially from space-based platforms like the *James Webb Space Telescope* (JWST) [128, 129], FINESSE [130], or EChO [131] could help resolve this issue.
- *Orbital phase curves for HD 189733b at 3.6 and 4.5 μ m.* Knutson et al. [126] report phase-variation observations for HD 189733b over a full orbit that may have implications with respect to CO-CH₄ transport-induced quenching. They find that 3D circulation models that assume chemical equilibrium have spectral signatures that compare well to *Spitzer* photometric channel fluxes for conditions in the dayside atmosphere at or near the secondary eclipse, but that the models

considerably overpredict the flux in the $4.5\ \mu\text{m}$ channel on the nightside. Knutson et al. [126] suggest that this nightside behavior at $4.5\ \mu\text{m}$, plus generally insufficient model absorption at $4.5\ \mu\text{m}$ in transit simulations, could be a signature of CO quenching, such that more CO exists in the terminator and nighttime atmosphere than is predicted from equilibrium models. This trend is indeed the expected one for CO-CH₄ quenching, but it is not clear from the information provided in [126] how much of the carbon is tied up in CH₄ in their nightside equilibrium model atmosphere and/or whether the magnitude of the quenching effect would be sufficient to produce the observed behavior (and note that disequilibrium models of Line et al. [60], Moses et al. [62, 63], and Venot et al. [66] have a lower CH₄/CO ratio in general than is considered in the Knutson et al. [126] quench discussion), nor is it clear whether other bulk atmospheric model parameters such as a non-solar metallicity or C/O ratio could produce the described behavior. Therefore, although the observations are certainly suggestive of disequilibrium quenching effects, additional models that explore a more complete range of parameter space, as well as higher-spectral-resolution observations in the 1-5 μm region that could help separate contributions from CO and CH₄, would help place the claim of disequilibrium effects on a firmer foundation. The observed phase-curve behavior for HD 189733b at $3.6\ \mu\text{m}$ is also interesting in that the minimum-to-maximum brightness temperature range over the orbit is greater at $3.6\ \mu\text{m}$ than at $4.5\ \mu\text{m}$ [126], despite equilibrium expectations that the $3.6\ \mu\text{m}$ band should have weaker average opacity than the $4.5\ \mu\text{m}$ band and thus probe deeper atmospheric levels where the thermal structure is not as variable. Additional disequilibrium opacity sources such as HCN or quenched methane could be causing the $3.6\ \mu\text{m}$ channel to probe higher altitudes; however, the fact that the eclipse depth at $3.6\ \mu\text{m}$ corresponds to a larger brightness temperature than at $4.5\ \mu\text{m}$ [126] suggests that the $3.6\ \mu\text{m}$ channel does indeed probe deeper levels on the dayside, as expected, and the larger phase variations at $3.6\ \mu\text{m}$ then might involve opacity changes at deep levels, which are not predicted from disequilibrium models. Again, further explorations of parameter space are required before the interesting observed behavior can be better understood.

- *Large inferred CO₂ abundance on HD 189733b.* The HST/NICMOS secondary-eclipse observations of Swain et al. [33] seem to require an unexpectedly large abundance of CO₂ in the dayside atmosphere of HD 189733b [34, 132, 133], leading to the suggestion that the CO₂ is supplied by photochemical processes [34]. However, thermo/photochemical kinetics and transport models [60, 62, 66] predict only small high-altitude increases due to photochemistry in the otherwise low expected CO₂ equilibrium abundance. In fact, retrievals that are based on the Swain et al. [33] data [34, 132, 133] suggest that the inferred CO₂ abundance is greater than that of water on HD 189733b — a situation that is very unlikely in a hydrogen-dominated atmosphere even under disequilibrium conditions. Therefore, as is emphasized by Moses et al. [63], the HST/NICMOS secondary-eclipse data, if robust, suggest that either (a) some other molecule is responsible for the absorption attributed to CO₂, (b) the atmospheric metallicity of HD 189733b is extremely high (e.g., several thousand times solar to allow CO₂/H₂O ratios greater than 1, which seems inconsistent with the high H & He content indicated by the planet’s mass-radius relationship [37]), or (c) all the current photochemical models are missing a major mechanism that irreversibly converts H₂O and CO

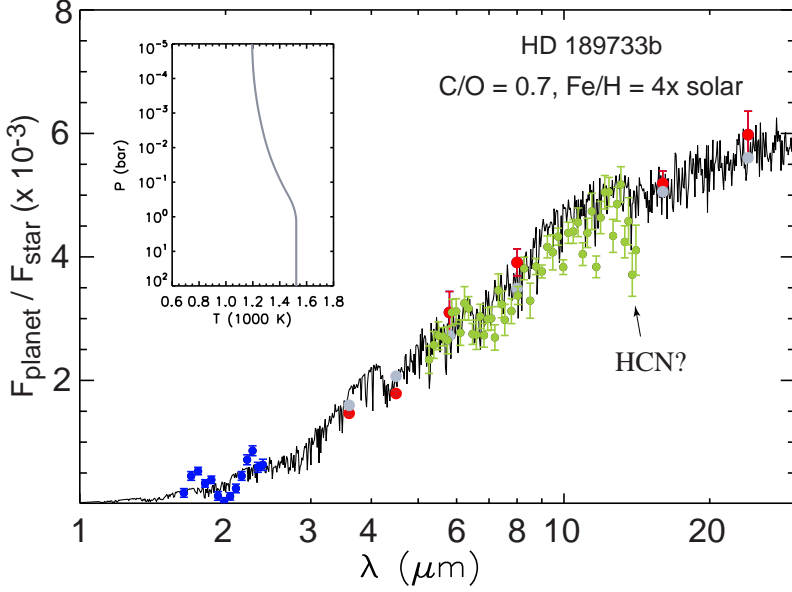


Figure 5. Synthetic eclipse spectra for HD 189733b from a Moses et al. [63] disequilibrium chemistry model that assumes a C/O ratio of 0.7 and a metallicity of $4\times$ solar (solid black line), compared with *Spitzer* broadband photometric points at 3.6 and 4.5 μm [126] and 5.6, 8, 16, and 24 μm [135, 125, 136] (large red circles with error bars), with *Spitzer* IRS spectra [29] (medium green circles with error bars), and with HST/NICMOS spectra [33] (small blue circles with error bars). The gray circles without error bars represent the model results convolved over the *Spitzer* broadband channels. The insert in the upper left shows the thermal profile adopted in the modeling (figure is modified from [63], with spectral calculations from N. Madhusudhan). Online version is in color.

into CO_2 (which seems unlikely in a hydrogen-dominated atmosphere). The Swain et al. [33] HST/NICMOS data therefore do not provide convincing evidence for disequilibrium process on HD 189733b, and some other factor must be at play here.

- *Spitzer/IRS absorption at $\sim 14 \mu\text{m}$ on HD 189733b.* *Spitzer/IRS* secondary eclipse spectra of HD 189733b [29] exhibit broad features consistent with water absorption in the 5–10 μm region on HD 189733b. Although not discussed by Grillmair et al. [29], the IRS spectra also exhibit a noticeable downturn at longer wavelengths that is suggestive of a ~ 13.5 – $14.5 \mu\text{m}$ absorption band, whereas *Spitzer* IRS and MIPS broadband photometric observations at 16 and 24 μm [136] jump back to higher brightness-temperature values. If the downturn in the flux at the longer wavelengths in the IRS spectrum is a real property of the atmosphere and not an observational artifact, we note from Fig. 5 that this behavior is reminiscent of a strong predicted $\sim 14 \mu\text{m}$ absorption feature due to HCN produced from thermochemical and photochemical kinetics in the disequilibrium models of Moses et al. [63] (see also [114]). This identification is certainly not definitive, and a more thorough investigation of model parameter space may suggest other alternatives, but we note that the HCN produced from disequilibrium process on HD 189733b is expected to survive throughout the atmosphere on both the dayside and nightside.

Searches for additional evidence for HCN on HD 189733b at other relevant wavelengths in transit and eclipse data might be worthwhile.

- *Relative 3.6-to-4.5- μm flux ratio on GJ 436b.* Broadband *Spitzer* secondary eclipse observations of the hot Neptune GJ 436b [122], and in particular the high observed flux at 3.6 μm in combination with the low flux (i.e., non-detection) at 4.5 μm , suggest that CO and not CH₄ is the dominant carbon constituent on the dayside of this cooler exoplanet, in serious conflict with chemical-equilibrium predictions [122, 86]. Stevenson et al. [122] and Madhusudhan & Seager [86] suggest that disequilibrium processes are responsible for this observed behavior, with transport-induced quenching in combination with a high metallicity (10 \times solar) producing the large required atmospheric CO and CO₂ abundances in the photosphere, and photochemistry removing the large expected large CH₄ abundance [86]. However, Line et al. [61] convincingly demonstrate that photochemistry cannot remove CH₄ from the bulk of the photosphere, and the thermal profiles derived from the general circulation models of Lewis et al. [110] for metallicities up to 50 \times solar do not predict a high-enough CO abundance at depth or anywhere else in the atmosphere for transport-induced quenching to supply the necessary CO mole fraction to the infrared photosphere [134]. Therefore, if the observations are robust, some process or atmospheric property other than transport-induced quenching and photochemistry must be responsible for the behavior, such as an extremely high metallicity [134] and/or high-altitude clouds, unless existing photochemical models are missing key mechanisms that efficiently convert water and methane to CO at relevant GJ 436b conditions.

The above discussions emphasize that many of the observational oddities that appear inconsistent with equilibrium chemistry in a near-solar-composition atmosphere also remain inconsistent with disequilibrium chemistry in such atmospheres. Photochemistry and transport-induced quenching are undoubtedly occurring on extrasolar giant planets, but the observational evidence gathered to date is not yet compelling, with the exception of CO quenching on young, directly imaged exoplanets. Certain atmospheric characteristics of hot Jupiters as described above, however, suggest that kinetic effects matter. Future observations are needed to help firm up these tantalizing hints of disequilibrium behavior; in the process, we will gain a better understanding of the underlying processes that control the planet's current atmospheric composition and its possible past and future evolution.

7. Conclusions

The ability to detect and characterize atmospheres of extrasolar planets represents a phenomenal success story in modern astronomy. We are, however, still in a learning phase, both in terms of the cutting-edge observational and analysis techniques needed to retrieve molecular abundances on hot Jupiters and in terms of theoretical models needed to interpret the observations. Disequilibrium chemistry models play an important role in the process. Photochemistry and transport-induced quenching will drive the exoplanet atmospheric compositions away from chemical equilibrium, and these effects will have observational consequences.

The main lessons learned to date from disequilibrium chemistry models are that transport-induced quenching is expected to affect the relative abundances of the carbon-bearing molecules CO and CH₄ and the nitrogen-bearing molecules N₂ and NH₃, which can have a notable impact on the transit, eclipse, and orbital-phase-variation observations in the spectral regions where these molecules have absorption bands. If the atmospheric thermal profile crosses the stability regimes where CO-CH₄ or N₂-NH₃ are stable in chemical equilibrium, the effects can be relatively major. If the thermal profile resides solidly within one regime or another, the effects can be subtle. Very hot planets will tend to kinetically maintain equilibrium, and disequilibrium effects will be confined to very high altitudes, except perhaps where the hotter parcels of gas are rapidly transported to cooler terminator or nightside regions. On warm to moderately hot Jupiters, H₂O and CO will remain at near-equilibrium abundances throughout the infrared photosphere, but transport-induced quenching will increase the abundance of CH₄ and NH₃ above equilibrium expectations. Further thermochemical and photochemical processing of the quenched CH₄ and NH₃ can lead to significant production of HCN (and in some cases C₂H₂), which can add opacity sources that fill in windows between water absorption bands. Carbon dioxide is relatively unaffected by disequilibrium chemistry but remains a very minor atmospheric constituent on hot Jupiters unless the atmospheric metallicity is significantly higher than solar. On cool exoplanets where methane is expected to be stable, transport-induced quenching can increase the expected abundance of CO, but photochemistry is not expected to remove methane from the troposphere and stratosphere. Methane and ammonia photochemistry on such planets will result in the production of complex hydrocarbons and nitriles that might produce high-altitude photochemical hazes. On exoplanets of a wide variety of temperatures, HCN and NH₃ will be important disequilibrium constituents that should not be ignored in observational analyses.

Higher-resolution infrared spectra from existing and future ground-based and space-based telescopes promise to provide the “smoking guns” needed to identify disequilibrium chemical constituents and their underlying kinetic controlling mechanisms.

Acknowledgment

This work was supported by the NASA Planetary Atmospheres Program grant number NNX11AD64G.

References

- 1 Deming, D., Seager, S. 2009. Light and shadow from distant worlds. *Nature* **462**, 301-306.
- 2 Seager, S. (Editor) 2010 *Exoplanets*. Tucson, AZ: Univ. Arizona Press.
- 3 Schneider, J., Le Sidaner, P., Savalle, R. & Zolotukhin, I. 2013. The Extrasolar Planets Encyclopaedia. See <http://exoplanet.eu/catalog/>.
- 4 Borucki, W. J., Koch, D. G., Basri, G., Batalha, N., Brown, T. M., Bryson, S. T., Caldwell, D., Christensen-Dalsgaard, J., Cochran, W. D., DeVore, E., et al. 2011. Characteristics of planetary candidates observed by Kepler. II. Analysis of the first four months of data. *Astrophys. J.* **736**, 19.
- 5 Batalha, N., Rowe, J. F., Bryson, S. T., Barclay, T., Burke, C. J., Caldwell, D. A., Christiansen, J. L., Mullally, F., Thompson, S. E., Brown, T. M., et al. 2012. arXiv:1202.5852.

- 6 Kalas, P., Graham, J. R., Chiang, E., Fitzgerald, M. P., Clampin, M., Kite, E. S., Stapelfeldt, K., Marois, C., Krist, J. 2008. Optical images of an exosolar planet 25 light-years from Earth. *Science* **322**, 1345-1348.
- 7 Marois, C., Macintosh, B., Barman, T., Zuckerman, B., Song, I., Patience, J., Lafrenière, D., Doyon, R. 2008. Direct imaging of multiple planets orbiting the star HR 8799. *Science* **322**, 1348-1352.
- 8 Traub, W. A. & Oppenheimer, B. R. 2010. Direct imaging of exoplanets. In *Exoplanets* (S. Seager, Editor), pp. 111-156, Tucson, AZ: Univ. Arizona Press.
- 9 Charbonneau, D., Brown, T. M., Noyes, R. W., Gilliland, R. L. 2002. Detection of an extrasolar planet atmosphere. *Astrophys. J.* **568**, 377-384.
- 10 Charbonneau, D., Allen, L. E., Megeath, S. T., Torres, G., Alonso, R., Brown, T. M., Gilliland, R. L., Latham, D. W., Mandushev, G., O'Donovan, F. T., Sozzetti, A. 2005. Detection of thermal emission from an extrasolar planet. *Astrophys. J.* **626**, 523-529.
- 11 Deming, D., Seager, S., Richardson, L. J., Harrington, J. 2005. Infrared radiation from an extrasolar planet. *Nature* **434**, 740-743.
- 12 Seager, S. & Deming, D. 2010. Exoplanet atmospheres. *Ann. Rev. Astron. Astrophys.* **48**, 631-672.
- 13 Hinz, P. M., Rodigas, T. J., Kenworthy, M. A., Sivanandam, S., Heinze, A. N., Mamajek, E. E., Meyer, M. R. 2010. Thermal infrared MMTAO observations of the HR 8799 planetary system. *Astrophys. J.* **716**, 417-426.
- 14 Bowler, B. P., Liu, M. C., Dupuy, T. J., & Cushing, M. C. 2010. Near-infrared spectroscopy of the extrasolar planet HR 8799b. *Astrophys. J.* **723**, 850-868.
- 15 Janson, M., Bergfors, C., Goto, M., Brandner, W., Lafrenière, 2010. Spatially resolved spectroscopy of the exoplanet HR 8799 c. *Astrophys. J.* **710**, L35-L38.
- 16 Currie, T., et al. 2011. A combined Subaru/VLT/MMT 1-5 μm study of planets orbiting HR 8799: Implications for atmospheric properties, masses, and formation. *Astrophys. J.* **729**, 128.
- 17 Barman, T. S., Macintosh, B., Konopacky, Q. M., Marois, C. 2011. Clouds and chemistry in the atmosphere of extrasolar planet HR8799b. *Astrophys. J.* **733**, 65.
- 18 Barman, T. S., Macintosh, B., Konopacky, Q. M., Marois, C. 2011. The young planet-mass object 2M1207b: A cool, cloudy, and methane-poor atmosphere. *Astrophys. J.* **735**, L39.
- 19 Madhusudhan, N., Burrows, A., Currie, T. 2011. Model atmospheres for massive gas giants with thick clouds: Application to the HR 8799 planets and predictions for future detections. *Astrophys. J.* **737**, 34.
- 20 Marley, M. S., Saumon, D., Cushing, M., Ackerman, A. S., Fortney, J. J., Freedman, R. 2012. Masses, radii, and cloud properties of the HR 8799 Planets. *Astrophys. J.* **754**, 135.
- 21 Konopacky, Q. M., Barman, T. S., Macintosh, B., Marois, C. 2013. Carbon and oxygen in the spectrum of HR 8799c. *Bull. Amer. Astron. Soc.* **221**, #126.03.
- 22 Vidal-Madjar, A., Lecavelier des Etangs, A., Désert, J.-M., Ballester, G. E., Ferlet, R., Hébrard, G., & Mayor, M. 2003. An extended upper atmosphere around the extrasolar planet HD209458b. *Nature* **422**, 143-146.
- 23 Vidal-Madjar, A., et al. 2004. Detection of oxygen and carbon in the hydrodynamically escaping atmosphere of the extrasolar planet HD 209458b. *Astrophys. J.* **604**, L69-L72.
- 24 Linsky, J. L., Yang, H., France, K., Froning, C. S., Green, J. C., Stocke, J. T., & Osterman, S. N. 2010. Observations of mass loss from the transiting exoplanet HD 209458b. *Astrophys. J.* **717**, 1291-1299.
- 25 Fossati, L., Haswell, C. A., Froning, C. S., Hebb, L., Holmes, S., Kolb, U., Helling, C., Carter, A., Wheatley, P., Collier Cameron, A. et al. 2010. Metals in the exosphere of the highly irradiated planet WASP-12b. *Astrophys. J.* **714**, L222-L227.
- 26 Sing, D. K., Désert, J.-M., Fortney, J. J., Lecavelier des Etangs, A., Ballester, G. E., Cepa, J., Ehrenreich, D., López-Morales, M., Pont, F., Shabram, M., Vidal-Madjar, A. 2011. Gran Telescopio Canarias OSIRIS transiting exoplanet atmospheric survey: Detection of potassium in XO-2b from narrowband spectrophotometry. *Astron. Astrophys.* **527**, A73.
- 27 Tinetti, G., et al. 2007. Water vapour in the atmosphere of a transiting extrasolar planet. *Nature* **448**, 169-171.
- 28 Barman, T. 2007. Identification of absorption features in an extrasolar planet atmosphere. *Astrophys. J.* **661**, L191-L194.
- 29 Grillmair, C. J., Burrows, A., Charbonneau, D., Armus, L., Stauffer, J., Meadows, V., van Cleve, J., von

- Braun, K., Levine, D. 2008. Strong water absorption in the dayside emission spectrum of the planet HD189733b. *Nature* **456**, 767-769.
- 30 Beaulieu, J. P., Carey, S., Ribas, I., & Tinetti, G. 2008. Primary transit of the planet HD 189733b at 3.6 and 5.8 μm . *Astrophys. J.* **677**, 1343-1347.
- 31 Swain, M. R., Vasisht, G., & Tinetti, G. 2008. The presence of methane in the atmosphere of an extrasolar planet. *Nature* **452**, 329-331.
- 32 Swain, M. R., et al. 2009. Water, methane, and carbon dioxide present in the dayside spectrum of the exoplanet HD 209458b. *Astrophys. J.* **704**, 1616-1621.
- 33 Swain, M. R., Vasisht, G., Tinetti, G., Bouwman, J., Chen, P., Yung, Y., Deming, D., Deroo, P. 2009. Molecular signatures in the near-infrared dayside spectrum of HD 189733b. *Astrophys. J.* **690**, L114-L117.
- 34 Madhusudhan, N., & Seager, S. 2009. A temperature and abundance retrieval method for exoplanet atmospheres. *Astrophys. J.* **707**, 24-39.
- 35 Désert, J.-M., Lecavelier des Etangs, A., Hébrard, G., Sing, D.K., Ehrenreich, D., Ferlet, R., & Vidal-Madjar, A. 2009. Search for carbon monoxide in the atmosphere of the transiting exoplanet HD 189733b. *Astrophys. J.* **699**, 478-485.
- 36 Snellen, I. A. G., de Kok, R. J., de Mooij, E. J. W., Albrecht, S., 2010. The orbital motion, absolute mass and high-altitude winds of exoplanet HD209458b. *Nature* **465**, 1049-1051.
- 37 Marley, M. S., Fortney, J., Seager, S., Barman, T. 2007. Atmospheres of extrasolar giant planets. In *Protostars and Planets V* (B. Reipurth, D. Jewitt, K. Keil, Editors), pp. 733-747, Tucson, AZ: Univ. Arizona Press.
- 38 Seager, S. & Sasselov, D. 1998. Extrasolar giant planets under strong stellar irradiation. *Astrophys. J.* **502**, L157-L161.
- 39 Burrows, A. & Sharp, C. M. 1999. Chemical equilibrium abundances in brown dwarf and extrasolar giant planet atmosphere. *Astrophys. J.* **512**, 843-863.
- 40 Marley, M. S., Gelino, C., Stephens, D., Lunine, J. I., Freedman, R. 1999. Reflected spectra and albedos of extrasolar giant planets. I. Clear and cloudy atmospheres. *Astrophys. J.* **513**, 879-893.
- 41 Ackerman, A. S. & Marley, M. S. 2001. Precipitating condensation clouds in substellar atmospheres. *Astrophys. J.* **556**, 872-884.
- 42 Lodders, K., & Fegley, B., Jr. 2002. Atmospheric chemistry in giant planets, brown dwarfs, and low-mass dwarf stars. I. Carbon, nitrogen, and oxygen. *Icarus* **155**, 393-424.
- 43 Sudarsky, D., Burrows, A., Hubeny, I. 2003. Theoretical spectra and atmospheres of extrasolar giant planets. *Astrophys. J.* **588**, 1121-1148.
- 44 Barman, T. S., Hauschildt, P. H., Allard, F. 2005. Phase-dependent properties of extrasolar planet atmospheres. *Astrophys. J.* **632**, 1132-1139.
- 45 Iro, N., Bézard, B., Guillot, T. 2005. A time-dependent radiative model for HD 209458b. *Astron. Astrophys.* **436**, 719-727.
- 46 Fortney, J. J., Lodders, K., Marley, M. S., Freedman, R. S. 2008. A unified theory for the atmospheres of hot and very hot Jupiters: Two classes of irradiated atmospheres. *Astrophys. J.* **678**, 1419-1435.
- 47 Prinn, R. G., & Barshay, S. S. 1977. Carbon monoxide on Jupiter and implications for atmospheric convection. *Science* **198**, 1031-1034.
- 48 Barshay, S. S., & Lewis, J. S. 1978. Chemical structure of the deep atmosphere of Jupiter. *Icarus* **33**, 593-611.
- 49 Lewis, J. S., & Fegley, M. B., Jr. 1984. Vertical distribution of disequilibrium species in Jupiter's troposphere. *Space Sci. Rev.* **39**, 163-192.
- 50 Moses, J. I., Fouchet, T., Bézard, B., Gladstone, G. R., Lellouch, E., Feuchtgruber, H. 2005. Photochemistry and diffusion in Jupiter's stratosphere: Constraints from ISO observations and comparisons with other giant planets. *J. Geophys. Res.* **110**, E08001. (doi:10.1029/2005JE002411)
- 51 Yelle, R. V., Griffith, C. A., Young, L. A. 2001. Structure of the Jovian stratosphere at the Galileo probe entry site. *Icarus* **152**, 331-346.
- 52 Karkoschka, E., & Tomasko, M. 2005. Saturn's vertical and latitudinal cloud structure 1991 2004 from HST imaging in 30 filters. *Icarus* **179**, 195-221.
- 53 Friedson, A. J., & Moses, J. I. 2012. General circulation and transport in Saturn's upper troposphere and

- stratosphere. *Icarus* **218**, 861-875.
- 54 Liang, M.-C., Parkinson, C. D., Lee, A. Y. T., Yung, Y. L., & Seager, S. 2003. Source of atomic hydrogen in the atmosphere of HD 209458b *Astrophys. J.* **596**, L247-L250.
 - 55 Liang, M.-C., Seager, S., Parkinson, C. D., Lee, A. Y. T., & Yung, Y. L. 2004. On the insignificance of photochemical hydrocarbon aerosols in the atmospheres of close-in extrasolar giant planets. *Astrophys. J.* **605**, L61-L64.
 - 56 Yelle, R. V. 2004. Aeronomy of extra-solar giant planets at small orbital distances. *Icarus* **170**, 167-179.
 - 57 García Muñoz, A. 2007. Physical and chemical aeronomy of HD 209458b. *Planet. Space Sci.* **55**, 1426-1455.
 - 58 Koskinen, T. T., Aylward, A. D., Smith, C. G. A., & Miller, S. 2007. A thermospheric circulation model for extrasolar giant planets. *Astrophys. J.* **661**, 515-526.
 - 59 Zahnle, K., Marley, M. S., Freedman, R. S., Lodders, K., & Fortney, J. J. 2009. Atmospheric sulfur photochemistry on hot Jupiters. *Astrophys. J.* **701**, L20-L24.
 - 60 Line, M. R., Liang, M. C., & Yung, Y. L. 2010. High-temperature photochemistry in the atmosphere of HD 189733b. *Astrophys. J.* **717**, 496-502.
 - 61 Line, M. R., Vasisht, G., Chen, P., Angerhausen, D., & Yung, Y. L. 2011. Thermochemical and photochemical kinetics in cooler hydrogen-dominated extrasolar planets: A methane-poor GJ 436b? *Astrophys. J.* **738**, 32.
 - 62 Moses, J. I., Visscher, C., Fortney, J. J., Showman, A. P., Lewis, N. K., Griffith, C. A., Klippenstein, S. J., Shabram, M., Friedson, A. J., Marley, M. S., Freedman, R. S. 2011. Disequilibrium carbon, oxygen, and nitrogen chemistry in the atmospheres of HD 189733b and HD 209458b. *Astrophys. J.* **737**, 15.
 - 63 Moses, J. I., Madhusudhan, N., Visscher, C., Freedman, R. S. 2013. Chemical consequences of the C/O ratio on hot Jupiters: Examples from WASP-12b, CoRoT-2b, XO-1b, and HD 189733b. *Astrophys. J.* **763**, 25.
 - 64 Miller-Ricci Kempton, E., Zahnle, K., & Fortney, J. J. 2012. The atmospheric chemistry of GJ 1214b: Photochemistry and clouds. *Astrophys. J.* **745**, 3.
 - 65 Kopparapu, R. K., Kasting, J. F., & Zahnle, K. J. 2012. A photochemical model for the carbon-rich planet WASP-12b. *Astrophys. J.* **745**, 77.
 - 66 Venot, O., Hébrard, G., Agúndez, M., Dobrijevic, M., Selsis, F., Hersant, F., Iro, N., & Bounaceur, R. 2012. A chemical model for the atmosphere of hot Jupiters. *Astron. Astrophys.* **546**, A43.
 - 67 Cooper, C. S., & Showman, A. P., 2006. Dynamics and disequilibrium carbon chemistry in hot Jupiter atmospheres, with application to HD 209458b. *Astrophys. J.* **649**, 1048-1063.
 - 68 Visscher, C., Lodders, K., & Fegley, B., Jr. 2006. Atmospheric chemistry in giant planets, brown dwarfs, and low-mass dwarf stars. II. Sulfur and phosphorus. *Astrophys. J.* **648**, 1181-1195.
 - 69 Fortney, J. J., Cooper, C. S., Showman, A. P., Marley, M. S., & Freedman, R. S. 2006. The influence of atmospheric dynamics on the infrared spectra and light curves of hot Jupiters. *Astrophys. J.* **652**, 746-757.
 - 70 Hubeny, I., & Burrows, A. 2007. A systematic study of departures from chemical equilibrium in the atmospheres of substellar mass objects. *Astrophys. J.* **669**, 1248-1261.
 - 71 Visscher, C., & Moses, J. I. 2011. Quenching of carbon monoxide and methane in the atmospheres of cool brown dwarfs and hot Jupiters. *Astrophys. J.* **738**, 72.
 - 72 Agúndez, M., Venot, O., Iro, N., Selsis, F., Hersant, F., Hébrard, E., & Dobrijevic, M. 2012. The impact of atmospheric circulation on the chemistry of the hot Jupiter HD 209458b. *Astron. Astrophys.* **548**, A73.
 - 73 Fegley, B., Jr., & Prinn, R. G. 1985. Equilibrium and nonequilibrium chemistry of Saturn's atmosphere: Implications for the observability of PH₃, N₂, CO, and GeH₄. *Astrophys. J.* **299**, 1067-1078.
 - 74 Yung, Y. L., Drew, W. A., Pinto, J. P., & Friedl, R. R. 1988. Estimation of the reaction rate for the formation of CH₃O from H + H₂CO: Implications for chemistry in the solar system. *Icarus* **73**, 516-526.
 - 75 Fegley, B., Jr., & Lodders, K. 1994. Chemical models of the deep atmospheres of Jupiter and Saturn. *Icarus* **110**, 117-154.
 - 76 Bézard, B., Lellouch, E., Strobel, D., Maillard, J.-P., Drossart, P. 2002. Carbon monoxide on Jupiter: Evidence for both internal and external sources. *Icarus* **159**, 95-111.
 - 77 Visscher, C., Moses, J. I., & Saslow, S. A. 2010. The deep water abundance on Jupiter: New constraints

- from thermochemical kinetics and diffusion modeling. *Icarus* **209**, 602-615.
- 78 Fegley, B., Jr., & Lodders, K. 1996. Atmospheric chemistry of the brown dwarf Gliese 229B: Thermochemical equilibrium predictions. *Astrophys. J.* **472**, L37-L39.
 - 79 Noll, K. S., Geballe, T. R., & Marley, M. S. 1997. Detection of abundant carbon monoxide in the brown dwarf Gliese 229B. *Astrophys. J.* **489**, L87-L90.
 - 80 Griffith, C. A., & Yelle, R. V. 1999. Disequilibrium chemistry in a brown dwarf's atmosphere: Carbon monoxide in Gliese 229B. *Astrophys. J.* **519**, L85-L88.
 - 81 Saumon, D., Geballe, T. R., Leggett, S. K., Marley, M. S., Freedman, R. S., Lodders, K., Fegley, B., Jr., & Sengupta, S. K. 2000. Molecular abundances in the atmosphere of the T Dwarf GL 229B. *Astrophys. J.* **541**, 374-389.
 - 82 Leggett, S. K., Saumon, D., Marley, M. S., Geballe, T. R., Golimowski, D. A., Stephens, D., & Fan, X. 2007. 3.6-7.9 μm photometry of L and T dwarfs and the prevalence of vertical mixing in their atmospheres. *Astrophys. J.* **655**, 1079-1094.
 - 83 Geballe, T. R., Saumon, D., Golimowski, D. A., Leggett, S. K., Marley, M. S., & Noll, K. S. 2009. Spectroscopic detection of carbon monoxide in two late-type T dwarfs. *Astrophys. J.* **695**, 844-854.
 - 84 Stephens, D. C., Leggett, S. K., Cushing, M. C., Marley, M. S., Saumon, D., Geballe, T. R., Golimowski, D. A., Fan, X., Noll, K. S. 2009. The 0.8-14.5 μm spectra of mid-L to mid-T dwarfs: Diagnostics of effective temperature, grain sedimentation, gas transport, and surface gravity. *Astrophys. J.* **702**, 154-170.
 - 85 Burrows, A., Budaj, J., Hubeny, I. 2008. Theoretical spectra and light curves of close-in extrasolar giant planets and comparison with data. *Astrophys. J.* **678**, 1436-1457.
 - 86 Madhusudhan, N., & Seager, S. 2011. High metallicity and non-equilibrium chemistry in the dayside atmosphere of hot-Neptune GJ 436b. *Astrophys. J.* **729**, 41.
 - 87 Baulch, D. L., et al. 2005. Evaluated kinetic data for combustion modeling: Supplement II. *J. Phys. Chem. Ref. Data* **34**, 757-1397.
 - 88 Atkinson, R., Baulch, D. L., Cox, R. A., Crowley, J. N., Hampson, R. F., Hynes, R. G., Jenkin, M. E., Rossi, M. J., Troe, J. 2006. Evaluated kinetic and photochemical data for atmospheric chemistry: Volume II – gas phase reactions of organic species. *Atmos. Chem. Phys.* **6**, 3625-4055.
 - 89 Sander, S., Abbatt, J. P. D., Barker, J. R., Burkholder, J. B., Golden, D. M., Kolb, C. E., Kurylo, M. J., Moortgat, G. K., Wine, P. H., Huie, R. E., Orkin, V. L. 2011. Chemical kinetics and photochemical data for use in atmospheric studies. Evaluation Number 17. JPL Publication 10-6, Jet Propulsion Laboratory, Pasadena, CA. (<http://jpldataeval.jpl.nasa.gov>)
 - 90 Showman, A. P., Fortney, J. J., Lian, Y., Marley, M. S., Freedman, R. S., Knutson, H. A., Charbonneau, D. 2009. Atmospheric circulation of hot Jupiters: Coupled radiative-dynamical general circulation model simulations of HD 189733b and HD 209458b. *Astrophys. J.* **699**, 564-584.
 - 91 Hidaka, Y., Oki, T., Kawano, H., Higashihara, T. 1989. Thermal decomposition of methanol in shock waves. *J. Phys. Chem.* **93**, 7134-7139.
 - 92 Tsang, W., & Hampson, R. F. 1986. Chemical kinetic data base for combustion chemistry. Part I. Methane and related compounds. *J. Phys. Chem. Ref. Data* **15**, 1087-1279.
 - 93 Jasper, A. W., Klippenstein, S. J., Harding, L. B., & Ruscic, B. 2007. Kinetics of the reaction of methyl radical with hydroxyl radical and methanol decomposition. *J. Phys. Chem. A* **111**, 3932-3950.
 - 94 Lewis, J. S., & Prinn, R. G. 1980. Kinetic inhibition of CO and N₂ reduction in the solar nebula. *Astrophys. J.* **238**, 357-364.
 - 95 Prinn, R. G., & Olaguer, E. P. 1981. Nitrogen on Jupiter: A deep atmospheric source. *J. Geophys. Res.* **86**, 9895-9899.
 - 96 Saumon, D., Marley, M. S., Cushing, M. C., Leggett, S. K., Roellig, T. L., Lodders, K., & Freedman, R. S. 2006. Ammonia as a tracer of chemical equilibrium in the T7.5 dwarf Gliese 570D. *Astrophys. J.* **647**, 552-557.
 - 97 Moses, J. I., Visscher, C., Keane, T. C., & Sperier, A. 2010. On the abundance of non-cometary HCN on Jupiter. *Faraday Disc.* **147**, 103-136.
 - 98 Klippenstein, S. J., Harding, L. B., Ruscic, B., Sivaramakrishnan, N. K., Su, M.-C., & Michael, J. V. 2009. Thermal decomposition of NH₂OH and subsequent reactions: Ab initio transition state theory and related shock tube experiments. *J. Phys. Chem. A* **113**, 10241-10259.

- 99 Dean, A. M., & Bozzelli, J. W. 2000. Combustion chemistry of nitrogen. In *Gas Phase Combustion Chemistry*, (W. C. Gardiner, Jr., editor), pp. 125-341, New York, NY: Springer-Verlag.
- 100 Hwang, D.-Y., & Mebel, A. M., 2003. Reaction mechanism of N_2/H_2 conversion to NH_3 : A theoretical study. *J. Phys. Chem. A* **107**, 2865-2874.
- 101 Asatryan, R., Bozzelli, J. W., da Silva, G., Swinnen, S., Nguyen, M. T. 2010. Formation and decomposition of chemically activated and stabilized hydrazine. *J. Phys. Chem. A* **114**, 6235-6249.
- 102 Stothard, N., Humpfer, R., Grotheer, H.-H. 1995. The multichannel reaction $NH_2 + NH_2$ at ambient temperature and low pressures. *Chem. Phys. Lett.* **240**, 474-480.
- 103 Konnov, A. A., & De Ruyck, J. 2000. Kinetic modeling of the thermal decomposition of ammonia. *Combust. Sci. and Tech.* **152**, 23-37.
- 104 Konnov, A. A., & De Ruyck, J. 2001. Kinetic modeling of the decomposition and flames of hydrazine. *Combust. Flame* **124**, 106-126.
- 105 Dean, A. M., Chou, M.-S., & Stern, D. 1984. Kinetics of rich ammonia flames. *Int. J. Chem. Kinetics* **16**, 633-653.
- 106 Dove, J. E., & Nip, W. S. 1979. Shock-tube study of ammonia pyrolysis. *Can. J. Chem.* **57**, 689-701.
- 107 Altinay, G., & Macdonald, R. G. 2012. Determination of the rate constant for the $NH_2(X^2B_1) + NH_2(X^2B_1)$ recombination reaction with collision partners He, Ne, Ar, and N_2 at low pressures and 296 K. Part 1. *J. Phys. Chem. A* **116**, 1353-1367.
- 108 Visscher, C. 2012. Chemical timescales in the atmospheres of highly eccentric exoplanets. *Astrophys. J.* **757**, 5.
- 109 Hu, R., Seager, S., Bains, W. 2012. Photochemistry in terrestrial exoplanet atmospheres. I. Photochemistry model and benchmark cases. *Astrophys. J.* **761**, 166.
- 110 Lewis, N. K., Showman, A. P., Fortney, J. J., Marley, M. S., Freedman, R. S., Lodders, K. 2010. Atmospheric circulation of eccentric hot Neptune GJ436b. *Astrophys. J.* **720**, 344-356.
- 111 Madhusudhan, N., et al. 2011. A high C/O ratio and weak thermal inversion in the atmosphere of exoplanet WASP-12b. *Nature* **469**, 64-67.
- 112 Visscher, C., Lodders, K., Fegley, B., Jr. 2010. Atmospheric chemistry in giant planets, brown dwarfs, and low-mass dwarf stars. III. Iron, magnesium, and silicon. *Astrophys. J.* **716**, 1060-1075.
- 113 Shabram, M., Fortney, J. J., Greene, T. P., Freedman, R. S. 2011. Transmission spectra of transiting planet atmospheres: Model validation and simulations of the hot Neptune GJ 436b for the James Webb Space Telescope. *Astrophys. J.* **727**, 65.
- 114 Madhusudhan, N. 2012. C/O ratio as a dimension for characterizing exoplanet atmospheres. *Astrophys. J.* **758**, 36.
- 115 Zahnle, K., Marley, M. S., Fortney, J. J. 2010. Thermospheric soots on warm Jupiters. arXiv:0911.0728v2.
- 116 Moses, J. I., Bézard, B., Lellouch, E., Gladstone, G. R., Feuchtgruber, H., Allen, M. 2000. Photochemistry of Saturn's atmosphere. I. Hydrocarbon chemistry and comparison to ISO observations. *Icarus* **143**, 244-298.
- 117 Fortney, J. J., Marley, M. S., Lodders, K., Saumon, D., Freedman, R. 2005. Comparative planetary atmospheres: Models of TrES-1 and HD 209458b. *Astrophys. J.* **627**, L69-L72.
- 118 Seager, S., Richardson, L. J., Hansen, B. M. S., Menou, K., Cho, J. Y.-K., Deming, D. 2005. On the dayside thermal emission of hot Jupiters. *Astrophys. J.* **632**, 1122-1131.
- 119 Kuchner, M. J., & Seager, S. 2005. Extrasolar carbon planets. arXiv:astro-ph/0504214.
- 120 Lodders, K. 2010. Exoplanet chemistry. In *Formation and Evolution of Exoplanets*, (R. Barnes, Ed.) Berlin: Wiley, 157.
- 121 Barman, T. S. 2008. On the presence of water and global circulation in the transiting planet HD 189733b. *Astrophys. J.* **676**, L61-L64.
- 122 Stevenson, K. B., et al. 2010. Possible thermochemical disequilibrium in the atmosphere of the exoplanet GJ 436b. *Nature* **464**, 1161-1164.
- 123 Madhusudhan, N., & Seager, S. 2010. On the inference of thermal inversions in hot Jupiter atmospheres. *Astrophys. J.* **725**, 261-274.
- 124 Fortney, J. J., Shabram, M., Showman, A. P., Lian, Y., Freedman, R. S., Marley, M. S., Lewis, N. K. 2010. Transmission spectra of three-dimensional hot Jupiter model atmospheres. *Astrophys. J.* **709**,

- 1396-1406.
- 125 Knutson, H. A., Charbonneau, D., Cowan, N. B., Fortney, J. J., Showman, A. P., Agol, E., Henry, G. W., Everett, M. E., Allen, L. E. 2009. Multiwavelength constraints on the day-night circulation patterns of HD 189733b. *Astrophys. J.* **690**, 822-836.
 - 126 Knutson, H. A., et al. 2012. 3.6 and 4.5 μm phase curves and evidence for non-equilibrium chemistry in the atmosphere of extrasolar planet HD 189733b. *Astrophys. J.* **754**, 22.
 - 127 Fortney, J. J., Marley, M. S., Saumon, D., Lodders, K. 2008. Synthetic spectra and colors of young giant planet atmospheres: Effects of initial conditions and atmospheric metallicity. *Astrophys. J.* **683**, 1104-1116.
 - 128 Gardner, J. P., et al. 2006. The James Webb Space Telescope. *Space Sci. Rev.* **123**, 485-606.
 - 129 Clampin, M. 2011. The James Webb Space Telescope and its capabilities for exoplanet science. In *The Astrophysics of Planetary Systems: Formation, Structure, and Dynamical Evolution*, Proceedings of the International Astronomical Union, IAU Symposium 276, 335-342.
 - 130 Swain, M. 2012. The FINESSE mission. American Astronomical Society, AAS Meeting #220, #505.05.
 - 131 Tinetti, G., et al. 2012. EChO. Exoplanet Characterisation Observatory. *Experimental Astron.* **34**, 311-353.
 - 132 Lee, J.-M., Fletcher, L. N., Irwin, P. G. J. 2012. Optimal estimation retrievals of the atmospheric structure and composition of HD 189733b from secondary eclipse spectroscopy. *Mon. Not. Royal Astron. Soc.* **420**, 170-182.
 - 133 Line, M. R., Zhang, X., Vashist, G., Natraj, V., Chen, P., Yung, Y. L. 2012. Information content of exoplanetary transit spectra: An initial look. *Astrophys. J.* **749**, 93.
 - 134 Richardson, M. R., Moses, J. I., Line, M. R., Barman, T. S., Visscher, C., Fortney, J. J. 2013. The effect of metallicity on the atmospheric composition of GJ 436b. 44th Lunar and Planetary Science Conference, 18-22 March 2013 in The Woodlands, TX, #2678.
 - 135 Knutson, H. A., Charbonneau, D., Allen, L. E., Fortney, J. J., Agol, E., Cowan, N. B., Showman, A. P., Cooper, C. S., Megeath, S. T. 2007. A map of the day-night contrast of the extrasolar planet HD 189733b. *Nature* **447**, 183-186.
 - 136 Charbonneau, D., Knutson, H. A., Barman, T., Allen, L. E., Mayor, M., Megeath, S. T., Queloz, D., Udry, S. 2008. The broadband infrared emission spectrum of the exoplanet HD 189733b. *Astrophys. J.* **686**, 1341-1348.